8-2014

Separation of single-walled carbon nanotubes by gel-based chromatography using surfactant step-gradient techniques and development of new instrumentation for studying SWCNT reaction processes

Leonard M. Breindel

Separation of single-walled carbon nanotubes by gel-based chromatography using surfactant step-gradient techniques and development of new instrumentation for studying SWCNT reaction processes

Leonard M. Breindel

B.S. Chemistry, State University of New York at Oswego, Oswego, NY, USA, 13126

A thesis submitted in partial fulfillment of the
requirements for the degree of Master of Science in Chemistry in the
School of Chemistry and Materials Science,
College of Science
Rochester Institute of Technology

August 2014

Signature of the Author _____

Accepted by _____

Director, M.S. Degree Program Date

SCHOOL OF CHEMISTRY AND MATERIALS SCIENCE
COLLEGE OF SCIENCE
ROCHESTER INSTITUTE OF TECHNOLOGY
ROCHESTER, NEW YORK

CERTIFICATE OF APPROVAL

M.S. DEGREE THESIS

The M.S. Degree Thesis of Leonard M. Breindel has
been examined and approved by the thesis
committee as satisfactory for the thesis required for
the M.S. degree in Chemistry.

_____

Dr. John-David R. Rocha, *Thesis Advisor*

_____

Dr. Christopher J. Collison, Committee Member

_____

Dr. Nathan C. Eddingsaas, Committee Member

_____

Dr. Reginald E. Rogers, Jr., Committee Member

_____

Date

ABSTRACT

Single-walled carbon nanotube (SWCNT) synthesis methods such as CoMoCAT™, HiPco™, pulsed laser vaporization (PLV), and catalytic chemical vapor deposition (CCVD) produce several different distributions of (*n*,*m*) SWCNT structures, where (*n*,*m*) defines the nanotube diameter and chiral wrapping angle. Post-synthesis processing such as functionalization and/or separations must therefore be employed to yield high purity electronic or single (*n*,*m*) samples. Through the use of a surfactant gradient across a gel-based chromatographic column, separations of single (*n*,*m*) species can be achieved. Anionic surfactants such as SDS, SDBS, and AOT display different separation effectiveness for single (*n*,*m*) species. Results of near-infrared optical absorption for separated SWCNT surfactant suspensions will be discussed, leading to a broader understanding of the important factors necessary for the gel chromatography separation technique. In particular, the effects of SWCNT/surfactant micelle structure are found to be key to achieving fast, simple SWCNT electronic type separations. Additionally, development of new instrumentation for the near-infrared spectrofluorimetric analysis (NIR-SFA) of SWCNTs is useful to the advancement of fundamental SWCNT research and applications. NIR-SFA, for instance, allows for the (*n*,*m*) structures of a sample to be identified and monitored during the progress of a chemical reaction or separation experiment. Seeking to achieve the time resolutions necessary for such experiments, the design and optimizations of a system utilizing single-wavelength excitation by diode lasers coupled with a fast NIR detection system are presented.

ACKNOWLEDGEMENTS

I would like to acknowledge several people that were vital in the completion of my research success at RIT. First I would like to acknowledge Dr. John-David Rocha, my research advisor, who gave me the opportunity to do research in his lab and provide guidance during my studies that allowed me to grow as a researcher. He provided me with the opportunity to present my research at two conferences and pushed me to work independently and showed me how to better my skills so that I may be a successful.

The member of my research committee have given me guidance during my studies that ensured I understand all aspects of my research and are able to convey my results in a way that is appropriate. Dr. Nathan Eddingsaas as well as serving on my committee offered me guidance when I was having trouble achieving emission with my instrument, through discussion about optics and help with my instrument Dr. Eddingsaas helped me greatly. Dr. Reginald Rogers provide me with an outside perspective that showed me how important it was to be able to clearly convey my work. Dr. Rogers also provided me we guidance not only in the direction of my research but also guidance in life outside of science. Dr. Christopher Collison although on sabbatical for a period of time during my studies provided me with guidance when it came to understanding the true purpose of my research and understand how important it is to understand what you are really trying to research. Dr. Collison also helped me understand the fundamental aspects of light absorption and emission of light.

Acknowledgement also must be made to Dr. Thomas Smith my research group with no only lab space and equipment to work with but also guidance in the role surfactants play in the separation of single-walled carbon nanotubes.

Finally I would like to acknowledge my family who provide me with moral support during my studies and encouragement when research was becoming overwhelming.

TABLE OF CONTENTS

ABSTRACT iii
ACKNOWLEDGEMENTS iv
TABLE OF CONTENTS vi
LIST OF FIGURES viii
CHAPTER 1 - INTRODUCTION 1
1.1 What is a single-walled carbon nanotube? 1
1.2 Geometric construction of SWCNTs 1
1.3 SWCNT production methods 3
1.3.1 *SWCNT production by solid/liquid/plasma catalysis* 4
1.3.2 *SWCNT production by chemical vapor deposition (CVD)* 6
1.4 SWCNT post-production techniques 7
1.5 SWCNT spectroscopic characterization techniques 10
1.5.1 *Raman spectroscopy* 12
1.5.2 *Absorbance spectroscopy* 13
1.5.3 *Fluorescence spectroscopy* 14
1.6 Uses of SWCNT fluorescence 16
1.6.1 *SWCNT kinetics* 17
1.7 Current Research Needs 19
CHAPTER 2 – INSTRUMENTATION FOR SWCNT FAST KINETIC ANALYSIS BY NEAR-INFRARED SPECTROFLUORIMETRY 20
2.1 Basics of spectrofluorimetry instrumentation 20
2.1.1 *Fluorescence of SWCNTs* 21
2.1.2 *SWCNT specific issues in classic spectrofluorimetry* 22
2.2 Modifying the classic fluorimeter for SWCNTs 23
2.3 New instrument 26
CHAPTER 3 – UNDERSTANDING OF INTERACTIONS LEADING TO SEPARATIONS OF METALLIC AND SEMICONDUCTINGSWCNT DISPERSIONS VIA STEP-GRADIENT GEL CHROMATOGRAPHY 38
3.1 Introduction 38
3.2 Experimental Methods 42

3.2.1 Sample Preparation 42
3.2.2 Chromatography 42
3.2.3 *Absorption spectroscopy* 43
3.3 Results and Discussion 43
3.3.1 Theory behind separation 43
3.3.2 Retention of semiconducting SWCNTs to Sephacryl gel 44
3.3.3 *Separation by SDS gradient* 46
3.3.4 Peak analysis of SDS fractions 49
3.3.5 Separation by SDBS gradient 52
3.3.6 Separation by AOT gradient 53
3.3.7 Peak analysis of AOT fractions 56
3.3.8 Implications of AOT 58
3.4 Conclusions 59
CHAPTER 4 – CONCLUSIONS AND FUTURE WORK 61
4.1 Conclusions 61
4.2 Future work 62
REFERENCES 65
APPENDIX 68
A1. LabVIEW code 68
A2. Plots of SWCNT separations using AOT at two different concentrations, 0.66 mM and 9 mM. 69
A3. SWeNT data sheets – SG65i 70

LIST OF FIGURES

Figure 1.1) Graphene sheet map of SWCNT (*n,m*) distribution

Figure 1.2) Laser pulse single-walled carbon nanotube production method

Figure 1.3) Arc discharge single-walled carbon nanotube production method

Figure 1.4) Chemical Vapor deposition single-walled carbon nanotube production method

Figure 1.5) Bundles of single-walled carbon nanotubes post production

Figure 1.6) Common surfactants used to isolate individual single-walled carbon naotubes from bundles

Figure 1.7) Density of states for metallic and semiconducting SWCNTs

Figure 1.8) Raman spectra of metallic and semiconducting SWCNTs

Figure 1.9) Absorbance spectra of metallic and semiconducting SWCNTs

Figure 1.10) Valence and conduction band for semiconducting SWCNTs

Figure 1.11) Diagram on SWCNTs used for the detection of nerve agents

Figure 2.1) Classic model of fluorometer with 90 degree detection angle

Figure 2.2) Experimental and computational spectra for single wavelength excitation

Figure 2.3) Diagram of instrument developed at Rice University by Rocha et al.

Figure 2.4) 2D fluorescence map of semiconducting SWCNT showing overlapping of emission at wavelengths 561 nm, 640 nm, 660 nm, and 730nm

Figure 2.5) Diagram of new instrument design

Figure 2.6) Image of sample holders constructed for instrument

Figure 2.7) Image of mirror mount constructed for instrument

Figure 2.8) Front panel of LabVIEW software for instrument

Figure 2.9) Illustration of how focusing mirror can improve detection of emitted light

Figure 2.10) Illustration of how sample holder can lead to decrease in detection

Figure 3.1) Separation of metallic and semiconducting SWCNTs

Figure 3.2) SDS gradient results

Figure 3.3) Separation of different *(n,m)* by SDS

Figure 3.4) Representative absorbance spectrum with simulated spectral data.

Figure 3.5) Summary of peak fitting for fractions with SDS gradient

Figure 3.6) Illustration of absorbance data for SDBS based gradient elution

Figure 3.7) AOT structure

Figure 3.8) Illustration of absorbance data for SDBS based gradient elution, top-non-normalized, bottom-normalized

Figure 3.9) Comparison of fractions collected from AOT gradient elution. The typical m-SWCNT fraction collected is also show for further comparison

Figure 3.10) Summary of peak fitting for fractions with AOT gradient, Pictures of fractions

Figure 3.11) AOT suspension and separation

CHAPTER 1 - INTRODUCTION

1.1 What is a single-walled carbon nanotube?

Single-walled carbon nanotubes (SWCNTs) are a nanostructure of carbon that has unique physical and electrical properties making it a topic of interest in many different fields of research ranging from alternative energy, to electrical wires, and uses for their textile strength.[1] When visualizing single-walled carbon nanotubes it is best to relate SWCNTs to graphene. When one thinks of a graphite pencil writing onto a sheet of paper, the pencil deposits several layers of graphene with each stroke of the pencil. If you were to remove one of these sheets of graphene and roll the sheet into a tube, one will have created a SWCNT.

1.2 Geometric construction of SWCNTs

SWCNTs vary in the diameter of the tube, ranging from 0.7 – 5.0 nm, but are commonly grown with diameters < 2 nm.[1-3] Diameter is one of the two attributes that result in the variation on physical and electrical properties, the other being chirality. When rolling the graphene sheet, the two edges of the graphene sheet have the ability to meet at a variety of different angles, sometimes resulting in chirality of the tube. This chirality of the SWCNT along with its diameter changes overlapping of the sp^2 hybridized carbons resulting in different electrical properties of SWCNTs.[4]

When considering a graphene sheet, SWCNTs can be characterized through vector components that will result in the rolling of different SWCNTs, these vectors give insight into the small differences in the diameter and chiral angle of the SWCNT. When considering a unit cell in a graphene sheet, the vectors from the center of the unit cell to the centers of the two adjacent cells can be considered R_1 and R_2. When rolling a

SWCNT from a graphene sheet, the sum of the number horizontal steps (n) and the number of vertical steps (m) results in the roll-up vector of the SWCNT (Equation 1.1).

$$R = n_1 R_1 + m_2 R_2 \qquad (1.1)$$

(n,m) vectors represent the difference in the conformation of the benzene rings in SWCNTs, "n" representing a zigzag conformation of the benzene rings while "m" representing the armchair configuration (Figure 1.1). From the (n,m) values, the diameter and chiral angle of the SWCNT can be calculated from equations 1.2 and 1.3.[5] For instance if we consider a SWCNT with an (n,m) of (9,4), then the chiral angle would be $\theta = 17.5^{\circ}$, and the diameter would be d = 0.916 nm (Fig. 1.1).

$$cos\,\theta = \frac{n+\frac{m}{2}}{\sqrt{n^2+nm+m^2}} \qquad (1.2)$$

$$d = \frac{a_o}{\pi}\sqrt{n^2 + nm + m^2} \qquad (1.3)$$

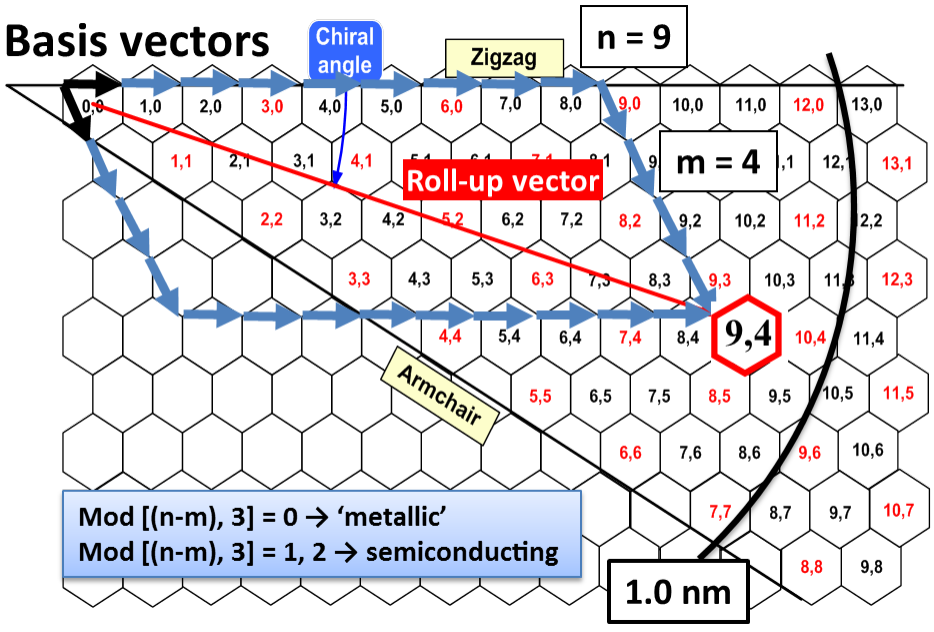

Figure 1.1 – A graphene sheet map, shows the different species of SWCNTs that result for a combination of the n and m values. (n,0) results in a zig-zag SWCNT that has a chiral angle of 0°, (n = m) results in an armchair SWCNT with a chiral angle of 30°. Two thirds of all SWCNTs are semiconducting, while only one third are metallic.

In any given sample of single-walled carbon nanotubes there are a variety nanotubes with different electrical properties.[6] SWCNTs fall into two different groups of electrical properties, nanotubes that have metallic electrical properties and nanotubes that have semiconducting electrical properties.[7] A general sample set of SWCNTs has a composition of 1/3 metallic SWCNTs and 2/3 semiconducting SWCNTs, indicated by the red and black hexagons, respectively, in Figure 1.1.[8] To determine the electric nature of a single carbon nanotube one can look at the (n,m) of each nanotube, if mod[(n-m),3] = 0 the SWCNT is metallic and mod[(n-m),3] $\neq$ 0 the SWCNT is semiconducting.[9] This rule allows for trends to be observed in the electronic properties, when $n = m$ the SWCNT is always in the armchair conformation and metallic in the electrical properties, when (n,0) the SWCNT is always in the zig-zag conformation but not always semiconducting.[10] For example, when examining the (7,1) – mod[(7-1),3] = 0, the SWCNT is metallic; while when examining (6,5) – mod[(6-5),3] = 1, the SWCNT is semiconducting. Large-scale production methods have yet to achieve the ability to specifically control the range of species of SWCNTs produced to a single type of either electronic character or (n,m)-species. An explanation of the common production techniques and their pros and cons are discussed in the next section.

1.3 SWCNT production methods

SWCNTs production can be broken down into two different groups: solid/liquid/plasma catalysis and chemical vapor deposition (CVD).[11] Two of the main methods of SWCNT production when considering solid/liquid/plasma catalysis are arc discharge and pulsed laser vaporization (PLV). These methods are based off the utilization of a solid carbon source, like a disk of graphite, that is embedded with

nanoparticles of a transition metal catalyst. Often in production, transition metals such as Fe, Co, and Ni are used.[12, 13]

1.3.1 *SWCNT production by solid/liquid/plasma catalysis*

Laser pulse production (Figure 1.2) is the first of the solid/laser/plasma methods to be discussed. Laser pulse production starts with the transition metal doped graphite disk being placed into a tube furnace filled with argon gas and raised to a temperature of ~1200 ^{0}C. When the transition metal doped graphite disk reaches the appropriate temperature a laser is pulsed into the graphite target, and in most cases, a frequency doubled 532 nm neodymium-doped yttrium aluminum garnet (Nd-YAG) laser is used.

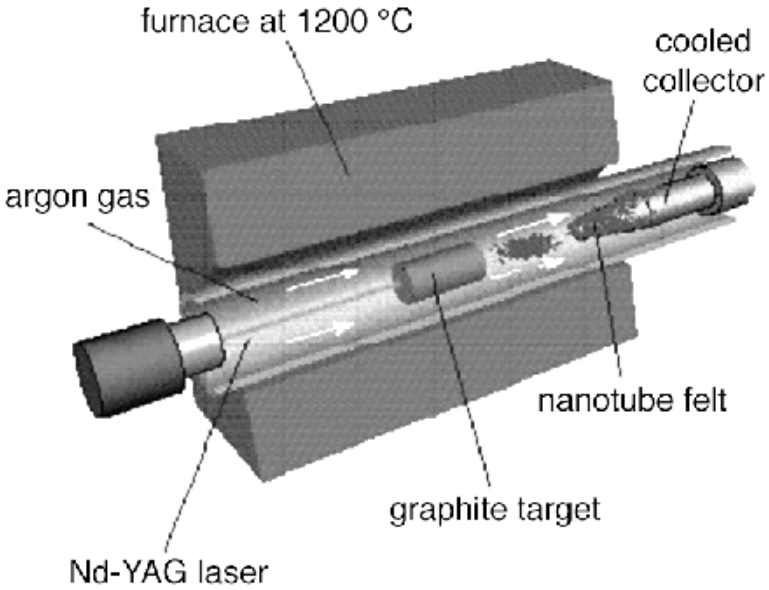

Figure 1.2 – The laser pulse production method was the first to discover SWCNTs in an attempt to better understand buckyballs.[14]

After impact by the laser on the disk, a highly charged solid-liquid-plasma is generated that results in excited carbon and metal catalyst particles ejected from the disk and flow down the tube. As the excited particles move down the tube they are attracted to the transition metal catalysts, forming six member rings leading to the growth of SWCNTs around the catalyst particles. Once reacted a cooling cone collects the newly formed

SWCNTs. While one tube is growing on one facet of a transition metal nanoparticle, other SWCNTs may also be growing on another facet. Grown tubes are collected on the cooled collecting cone for further processing. Laser pulse production typically produces SWCNTs with diameters ranging from 1.2 – 1.6 nm.[14]

The second form of solid/laser/plasma production methods is arc discharge production (Figure 1.3). Arc discharge uses the same transition metal doped graphite disk that is used in the laser pulse production method, but rather as the anode in the electrical circuit. With a second graphite disk as the cathode and an interelectrode gas containing helium (sometimes Ar or N_2), ionized carbon, and neutral carbon under pressure (660 mbar), a current of 100 A and voltage drop of 30 V is discharged across the cathode and anode. Ejected excited carbon atoms and transition metal nanoparticles form SWCNTs in the same manner as mentioned in the description of laser pulse production.[15] During production runs the transition metal doped graphite disk is rotated to allow for even ejecting of material. Arc discharge typically production produces SWCNTs with diameters that range from 1 – 1.4 nm.[1]

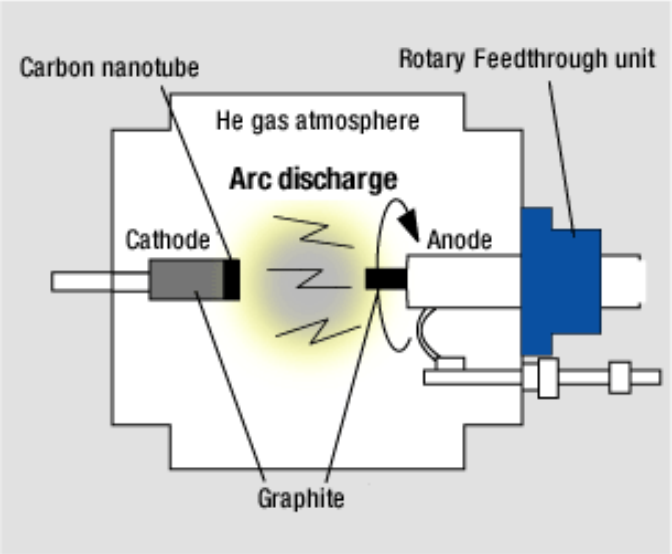

Figure 1.3 – Arc-discharge production.[16]

1.3.2 *SWCNT production by chemical vapor deposition (CVD)*

Production of SWCNTs by chemical vapor deposition (CVD) (Figure 1.4) differs from solid/laser/plasma production in that is based on the decomposition of gaseous or volatile compounds containing carbon.[17] Like solid/laser/plasma production, CVD production methods rely on the use of a transition metal catalyst such as Fe, Co, and Ni for the formation of SWCNTs. Production by CVD is not exclusive to the formation of SWCNTs, CVD also has the ability to produce multi-walled carbon nanotubes (MWCNTs) and other nanostructures of carbon such as graphene and Buckyballs (C_{60}).[2] CVD production has the ability to produce kg per day quantities and have better diameter control than solid/laser/plasma production methods.[11]

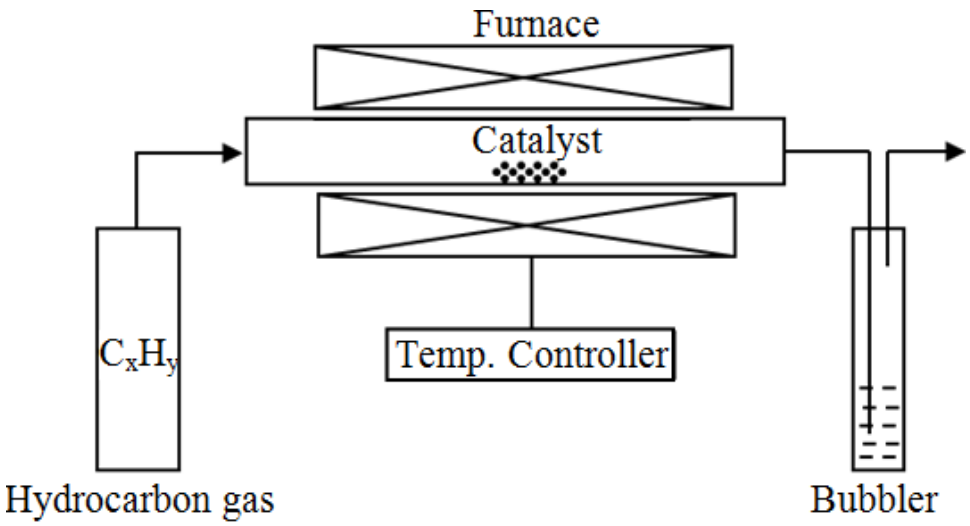

Figure 1.4 – Chemical vapor deposition (CVD) is a production method that utilized a hydrocarbon gas as a feed stock passing through a furnace with the catalyst stationary.[18]

The first of the two main production methods that utilize CVD is high pressure catalytic decomposition of carbon monoxide (HiPco). HiPco production is a high pressure method that operates at pressures around 30 – 50 atm and temperatures of 900 – 1100 $^{\circ}$C. HiPco works by passing a combination of cold carbon monoxide (CO) with a

catalyst source such as $Fe(CO)_5$ through a nozzle that will rapidly decompose the CO and catalyst source allowing for the formation of SWCNTs. To add to this decomposition, hot CO is added to the reaction at the nozzle to produce an additional carbon source. Metal catalysts used in HiPco and other CVD methods are the same metals that are used in solid/laser/plasma production. HiPco production generally yields SWCNTs with a diameter range of 0.8 – 1.2 nm.[2, 19]

The second CVD method for large-scale production is Co-Mo bimetallic catalyst (CoMoCAT). CoMoCAT works under the same ideas as HiPco with some changes to the method. CoMoCAT production operates at pressures of 1 – 10 atm and temperatures of 700 – 950 $^{\circ}$C. CoMoCAT also differs from HiPco in the way that it introduces the catalyst to the CO feedstock, HiPco is a floating catalyst method while CoMoCAT is a supported catalyst, embedding the catalyst in silica particles. This creates a fluidized bed as the catalyst is released into a flow of CO gas in the reactor.[20] CoMoCAT production offers a finer control on the diameter range, commonly 0.7 – 0.9 nm. This reduced diameter range results in a high control of (*n*,*m*) diversity in SWCNT samples.[3] CoMoCAT production can yield samples that are considered to be (6,5) enriched.[21]

1.4 SWCNT post-production techniques

After production of SWCNTs is complete the next step before the material can be used is the removal of the transition metal catalyst from the SWCNTs. This is most often achieved through a strong acid reflux. Nitric acid has shown to be efficient at removing up to 90% of non-tubular carbon and dissolves metal oxides leftover from the catalyst. For CoMoCAT produced SWCNTs, the removal of silica support is achieved through a hydrofluoric acid digest as silica represents 90 wt% of the collected materials. With the

nitric acid reflux and hydrofluoric acid digest working to remove unwanted material, it also oxidizes the SWCNTs creating COOH groups on the nanotube ends were the metal catalyst has been removed and along the length of the tube where an imperfection may have been removed. Removal of COOH groups is achieved by placing the SWCNTs into a furnace to burn off any imperfections.

To further our understanding of SWCNTs, photophysical properties can be investigated, First sample preparations must be employed. During the production process newly formed SWCNTs aggregate into bundles due to weak interactions to neighboring SWCNTS during production. Figure 1.5 illustrates a few examples of these SWCNT bundles for raw production materials from both the arc discharge method and the HiPco process. Bundles of SWCNTS have a negative effect in photophysical processes as they often lead to peak broadening. Peak broadening is a result of the excited state of one SWCNT being transferred to a neighboring SWCNT in a bundle; this can be due to absorbance of emitted light from neighboring SWCNTs and vibrational relaxation.[22] In order to be able to use photophysical properties to better understand SWCNTs, these bundles need to be separated.

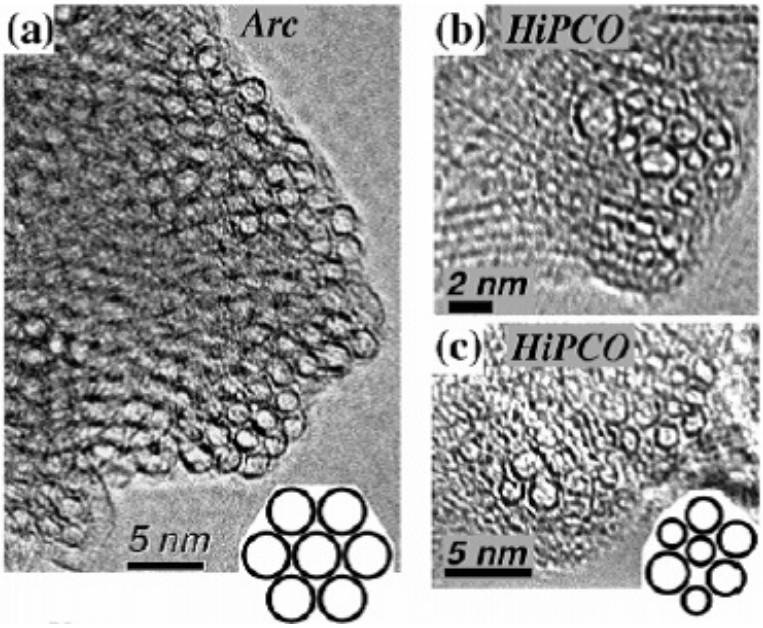

Figure 1.5 – Bungles of different sizes form during the SWCNT production process and have a negative effect on the photophysics of SWCNTs and it leads to peak broadening in absorbance and an inner filter effect during fluorescence.[23]

One method of breaking up the bundles is to place the SWCNTs in a surfactant that will allow for their separation or isolation. Commonly used surfactant is sodium dodecylsulfate (SDS), sodium dodecylbenzenesulfonate (SDBS), and sodium cholate (SC)(Figure 1.6). When the surfactant is sonicated in the presence of SWCNTs creates micelles around each of the SWCNTs. The micelle structure has the form of hydrophobic aliphatic tails of SDS and SDBS aligning with the tube sidewalls, or in the case of SC the carbon ring system lies flat on the tube surface, while the hydrophilic headgroups like sulfates or hydroxyls face outwards towards the aqueous solvent. As the surfactants begin to surround the SWCNTs during the sonication process, the van der Waals forces keeping the bundles together are broken and thus releasing individual tubes from larger bundles. After sonication, the suspension is next centrifuged to separate the newly isolated SWCNTs from the bundles of SWCNTs that the SDS was not able to break apart and any other nano-carbon structures that the post-production cleanup left behind.[22]

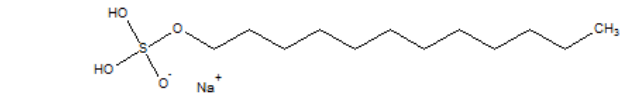

Sodium dodecyl sulfate

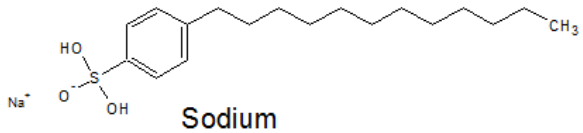

Sodium dodecylbenzenesulfonate

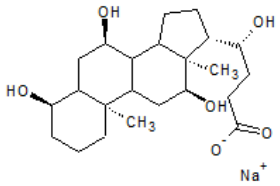

Sodium Cholate

Figure 1.6 – Structures of sodium dodecyl sulfate (SDS), sodium dodecylbenzenesulfonate (SDBS), and sodium cholate (SC).

After sonication and centrifugation, in order to use in some applications or to consider some SWCNT photophysical processes, metallic SWCNTs (m-SWCNTs) must be separated from semiconducting SWCNTs (sc-SWCNTs). Chromatography allows for separation of metallic from semiconducting through the use of a stationary phase such as Sephacryl-200 and a mobile phase of 1 wt% SDS.[24, 25] Metallic nanotubes elute from the column and result in a yellow-green fraction, while semiconducting SWCNTs elute second and result in a purple fraction. The dominant mechanism affording this electronic SWCNT type separation is still a significant research area, and thus methods to a enhance the process and gain further fundamental understanding are the thrusts of Chapter 3 in this thesis.

1.5 SWCNT spectroscopic characterization techniques

To better understand the photophysical properties that are involved in the characterization of SWCNTs it is easiest to think of the simplest model of the density of

states. SWCNTs are considered to be m-SWCNTs when an overlapping occurs between the occupied π and unoccupied π^* energy levels allowing electrons to freely move between all the energy levels resulting in conduction.[26] However in the case of sc-SWCNTs, the occupied π and unoccupied π^* orbitals do not overlap resulting in an energy gap. When considering the density of states (DOS) that indicate the number of available electron states at a given energy level, they show regions of extreme density of electrons in very discrete energy levels. These regions are known as van Hove singularities and reflect the 1D nature of SWCNTs.[5]

Spectroscopic transitions involve transitions from the valence and conduction band pairs often referred as $E_{jj.}$ Metallic SWCNTs exhibit a finite amount of electronic states at the Fermi level, while semiconducting SWCNTs result in forbidden regions of electron density between the conduction and valence bands often referred to as bandgaps. The energy of the bandgap is inversely dependent on the diameter of the SWCNT according to equation 1.4[26]

$$E_{jj} = 2ja_{C-C}\gamma_0/d_t \qquad (1.4)$$

where *j* is the transition index, a_{C-C} is the nearest neighbor C-C distance, γ_0 is the nearest neighbor interaction energy, and d_t is the nanotube diameter. m-SWCNTs generally result in an M_{11} region that lies between ~350 to ~490 nm. sc-SWCNTs usually show two main transitions, the S_{11} lying in the region of ~820 – 1700 nm and the S_{22} region lying between ~ 475 – 820 nm (Figure 1.7).[27]

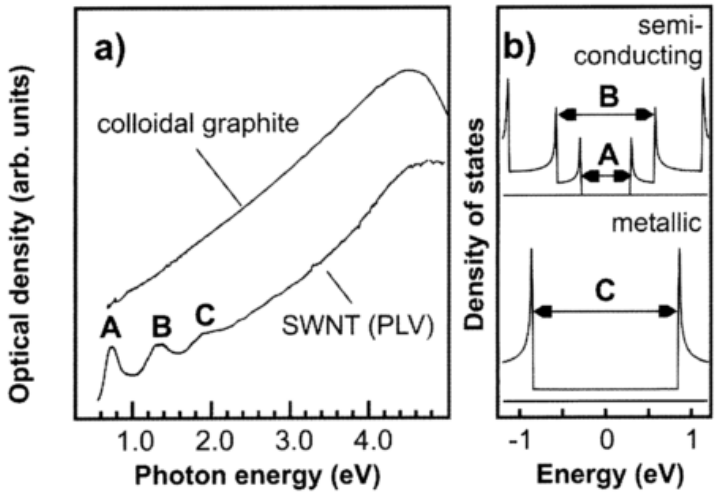

Figure 1.7 – Figure of density of states of metallic and semiconducting SWCNTs.[28]

1.5.1 *Raman spectroscopy*

Raman spectroscopy of SWCNTs has the ability to observe both m- and sc-SWCNTs, as Raman is an examination of the vibrational energy modes.[29] Raman spectra illustrate a number of important characteristic peak modes of SWCNTs, like the radial breathing mode (RBM), D-band, G-band, and G′-band (sometimes 2D) (Figure 1.8).[30] The RBM intensity of SWCNTs depends on the diameter and chiral angle of the different SWCNTs as well as if the SWCNT is metallic or semiconducting (Figure 1.7).[31] The ability to use Raman as a spectroscopy method of characterization for SWCNTs in a solution is difficult, since it relies heavily on the use of a highly monochromatic and powerful excitation laser.[32, 33] In order to be able to use Raman as a broad method of characterization of SWCNTs in solution, the laser excitation wavelengths must align strongly with the various SWCNT bandgaps to induce observable scattering. Since the RBM scattering peaks are the only discriminating peaks for SWCNT (*n*,*m*) or electronic type characterization and exhibit some of the weakest intensity transitions, one will have to incorporate a broadly tunable laser to have a full range of excitation wavelengths, or

several different excitation sources must be utilized to cover the appropriate range (~450 – 800 nm). Although both methods of providing multiple sources of excitation are possible, they would be proven to be extremely expensive and not cost efficient.[10]

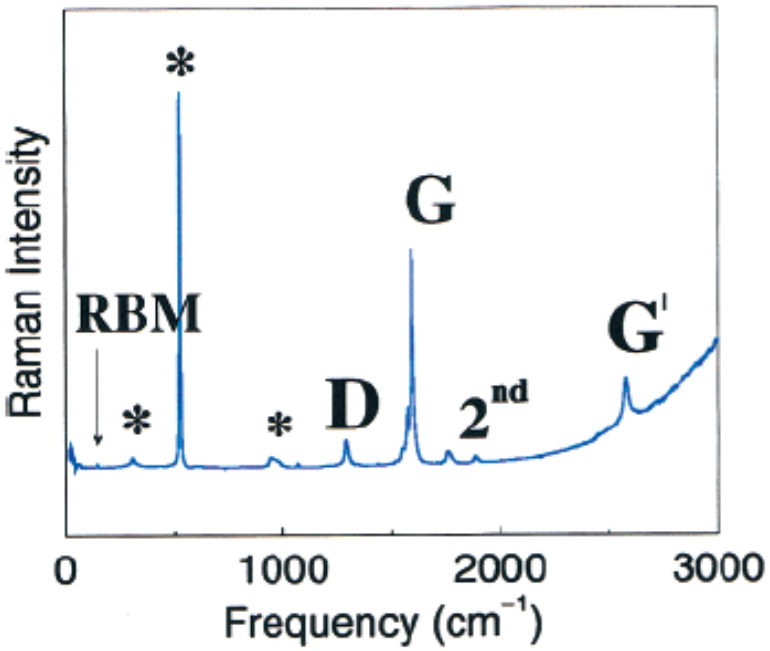

Figure 1.8 – Metallic and semiconducting SWCNT observable using raman spectroscopy. The different (*n*,*m*) can be identified through the radial breathing modes. D stands for the amount of diamond like structure that is present in the sample while G stands for the graphene portion of the sample.[34]

1.5.2 *Absorbance spectroscopy*

Absorbance spectroscopy has become a common instrumental technique for characterization of SWCNTs due to the ability of most commercial instruments to be outfitted with detectors that can observe light ranging from the ultra-violet all the way to the infrared.[35] Absorbance spectroscopy also has the ability to detect both metallic and semiconducting SWCNTs in a solution (Figure 1.9). But this method is not without its fall backs. One of the main fall backs is the inability to differentiate between different (*n*,*m*)-types in solution due to significant overlapping of the spectral peaks. If all of the SWCNTs in solution are not individual SWCNTs after the sonication and centrifugation

steps, any broken bundles, impurities, and SWCNTs with defects will result in a broadening of the peaks and a non-zero baseline.[36] As shown in Figure 1.9, absorbance can be used to monitor separation methods that aim to separate metallic from semiconducting SWCNTs, as the regions of metallic and semiconducting differ, but falls short when trying to separate SWCNTs by their different (*n*,*m*)-types.

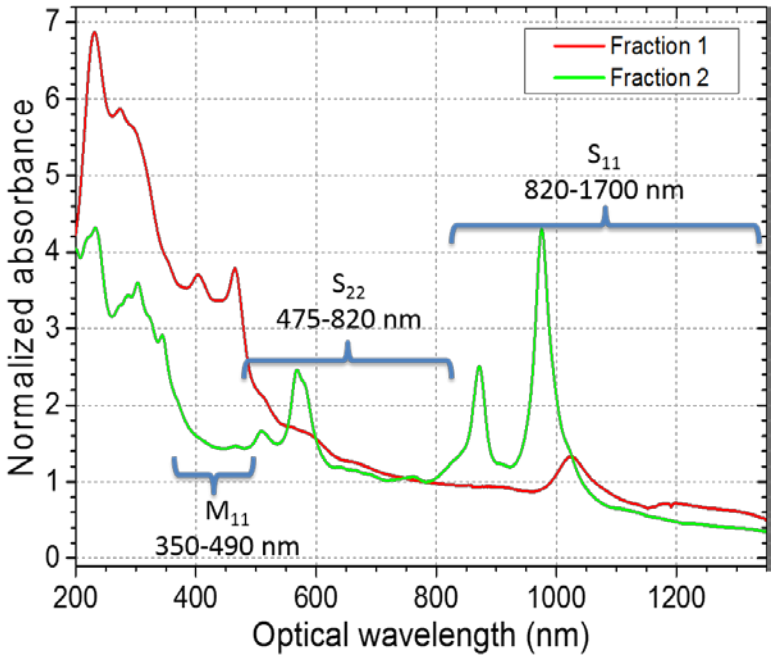

Figure 1.9 – Absorbance spectra of metallic and semiconducting fractions of separated SWCNTs. Fraction 1 has a stronger absorbance in the M_{11} region indicating a metallic fraction, fraction 2 shows better absorption in the S_{22} and S_{11} regions pointing to a semiconducting fraction.

1.5.3 *Fluorescence spectroscopy*

One method that has the ability to differentiate between the (*n*,*m*) of different SWCNTs in a solution is fluorescence spectroscopy.[37] Fluorescence spectroscopy is fairly new to SWCNT research as it was previously thought to be useless because emitted light is reabsorbed by neighboring SWCNTs before it has the ability to leave the bundle. With the addition of sonication and centrifugation to the preparation of samples used in optical studies, fluorescence is now a viable research tool.[8] Fluorescence spectroscopy

normally starts with the excitation of the SWCNT over the E_{22} bandgap, then emission occurs from the E_{11} bandgap (Figure 1.10). One can recall Kasha's rule, which states that emission of light will occur from the lowest conductive band to the highest valence band and is independent of excitation bandgap.[6] Two dimensional fluorescence mapping (excitation vs emission) of a solution of SWCNTs allows for the identification of different (*n*,*m*) SWCNT types.[6] When comparing cross sections of excitation and emission of a SWCNT to a study done by Weisman and Bachilo (Rice University) that calculated van Hove optical transitions of all SWCNTs between 0.48 and 2.0 nm, the identity of the different (*n*,*m*) species can be found.[9] Because fluorescence spectroscopy is dependent of the presence of a bandgap, metallic SWCNTs cannot be observed using this method.

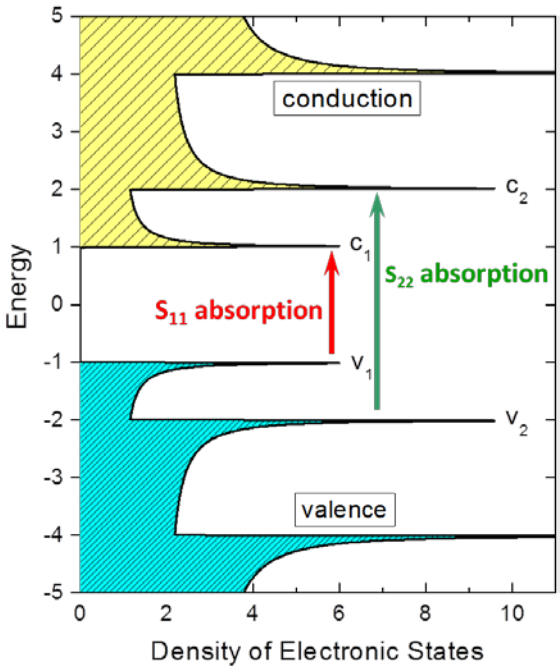

Figure 1.10 – A diagram of the density of states of the valence and conduction bands of semiconducting SWCNTs.[6]

1.6 Uses of SWCNT fluorescence

One interesting use of fluorescence when it comes to SWCNTs is the ability to use fluorescence to understand the kinetics of how well a SWCNT can be functionalized.[38] A functional group covalently attaching to a SWCNT sidewall disrupts the π-electron system and thus acts as a fluorescence quenching site, observable as a decrease in detected emission signal. Functionalization of SWCNTs is an important area of research because it allows SWCNTs to be used in commercial applications. Many of the current applications such as gas sensors, drug delivery, semiconductors, and even wires, requires the SWCNTs to be functionalized to some extent in order to better enhance the chemical or physical properties of the SWCNT. One example of this functionalization by Liu, Jinhuai et al. [39] at Anhui University is the addition of p-hexafluoro-isopropanol phenyl (HFIPPH) to SWCNTs that will allow for the detection of nerve agents through hydrogen bonds made between the HFIPPH and the nerve agent (Figure 1.11).

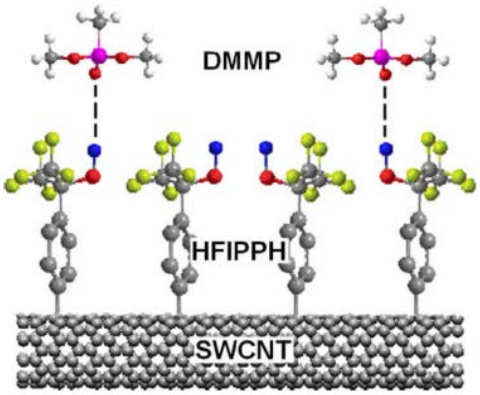

Figure 1.11 – SWCNT-HFIPPH with DMMP.[39]

A second interest in understanding the kinetics of SWCNTs is rooted in the need for a single chirality sample. For use as a semiconductor, SWCNTs must be split into their different electrical properties so they can be properly applied to a given task.

Current separation methods as previously discussed had the ability to separate metallic from semiconducting, but most fall short when moving towards single chirality. As will be discussed in Chapter 3, by investigating how a SWCNT interacts with the separation medium one can move towards applying appropriate separation methods to achieve single chirality.

1.6.1 *SWCNT kinetics*

To investigate the kinetics, real-time fluorescence spectroscopy can be used. By measuring the intensity of the fluorescence of the SWCNTs, functionalization can be monitored by observing emission quenching. Functionalization has a quenching effect of the SWCNT emission because as a ligand attaches to the walls of the SWCNT it confines a free electron to one position reducing the SWCNTs ability to fluoresce. Quenching effects often result in an exponential decay of fluorescence and can be on a rather short time scale, sub-millisecond down to potentially nanosecond timescales. This is significantly slower than average SWCNT fluorescence decay lifetimes that occur on the femtosecond and picosecond timescales.

To better understand the kinetics of real-time fluorescence quenching, a look at bimolecular kinetics when the quencher is in excess can be a good place to start.

$$A + B \rightarrow C \qquad (1.5)$$

In equation 1.5, *A* represents a free SWCNT in solution. We can assume that all free SWCNTs in solution will fluoresce, so we can call the concentration of SWCNTs equal to the intensity of the fluorescence, I_F. *B* represents the ligand to be attached to the SWCNT thus resulting in quenching. *C* is the newly functionalized SWCNT that does not

fluoresce. The rate law of the change in concentration of SWCNTs will look something like this:

$$\frac{\mathrm{d}[A]}{\mathrm{dt}} = -k[A][B] \tag{1.6}$$

Where *k* is the rate constant. Next, equation 1.6 is rearranged so that the equation will be in the form that will allow for the isolation of the change in concentration of SWCNTs.

$$\frac{\mathrm{d}[A]}{[A]} = -k[B]\mathrm{dt} \tag{1.7}$$

An integration of both sides of equation 1.7 from 0 to *A* and 0 to time, *t*, will result in equation 1.8:

$$\ln[A] = -k[B]t \tag{1.8}$$

The last step is to apply the exponential function to both sides of equation 1.8 so that the concentration of SWCNTs can be found with respect to time and concentration of quencher.

$$[A] = e^{-k[B]t} \tag{1.9}$$

Although SWCNT fluorescence quantum yields are low (< 10%), equation 1.9 can be written in respect to intensity of fluorescing SWCNTs as a monitor for the overall behavior of SWCNTs in a suspension:

$$I_{\mathrm{SWCNTs}} = e^{-k[B]t} \tag{1.10}$$

Since under constant excitation high quality SWCNTs typically do not exhibit emission blinking, a monitoring of fluorescence intensity over time will result in a constant signal. This would be the initial state of the system with [B] = 0. The addition of quencher would then be observed as an exponential decay of fluorescence. Using equation 1.8, the slope of the best fit line will be equal to the rate constant times the concentration of the ligand (quencher) initially added to the solution.

1.7 Current Research Needs

Presently studies of SWCNT separations have been hindered by the lack of fundamental mechanistic understandings. Much of the work has been focused on incremental improvements or methods modifications, however pushing the various techniques forward at large-scale will require the ability to know which parameters are relevant to monitor. This will be especially true for advanced applications that for instance may require > 99% purity of SWCNT (*n*,*m*) types.

This thesis will focus on two different aspects of this issue. To address the needs for experimental methods and apparatus to better understand SWCNT interactions with functional groups, Chapter 2 of this thesis will discuss the development of instrumentation that will assist in the understanding of these interactions. In Chapter 3, the focus shifts towards the separation of electronic SWCNT types in practice and developing an understanding of the role surfactants play.

CHAPTER 2 – INSTRUMENTATION FOR SWCNT FAST KINETIC ANALYSIS BY NEAR-INFRARED SPECTROFLUORIMETRY

2.1 Basics of spectrofluorimetry instrumentation

Classic fluorescence is a commonly used analytical technique that is used in many different areas of chemistry. A standard spectrofluorimeter is illustrated in Figure 2.1.

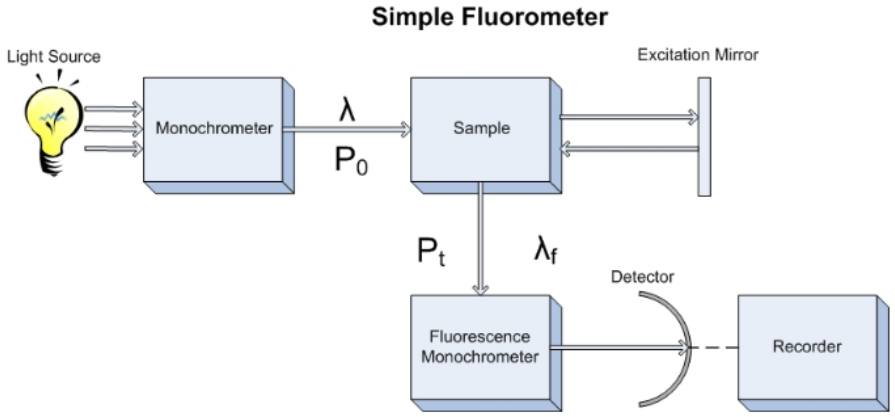

Figure 2.1 – A classic model of a fluorometer with a white light source and a 90 degree detection angle.

The basic operation of such an instrument is the following. A Xe-arc halogen lamp as an excitation source produces an array of wavelengths of light that can be used. One wavelength of interest is chosen by a monochromator, and this monochromatic light is now shined onto the entry window in the sample holder and excitation occurs in the sample. After the sample is excited, the emitted fluorescence scatters in 360º but exits the sample holder at a 90° angle from the excitation light and travels to a scanning monochromator. The 90° change in direction from the emission light from the excitation light is to minimize the amount of excitation light that might reach the detector. Emission spectra is red shifted from the absorption spectra generally with large amounts of overlapping between the two spectra so it is important to minimize the amount of excitation light that can reach the detector because it will place an error in the data. After the emission leaves the sample it is separated into the individual wavelengths that make

up the emission by a scanning monochromator. This allows for the unique characteristics of the fluorescence to be observed. After the scanning monochromator separates the emission by wavelength the light reaches the detector that measures the intensity.

2.1.1 *Fluorescence of SWCNTs*

The use of a classic fluorimeter in the study of SWCNTs allows for individual (*n,m*) in a sample to be determined. When looking at the emission spectrum of a sample of SWCNTs, the peaks found in the spectrum relate to individual (*n,m*) species of SWCNTs observed.[6] This was confirmed in a paper by J.-D. R. Rocha et al. where the Voigt functions of each (*n,m*) were calculated (Figure 2.2).[40] After calculating the Voigt functions the overlapping regions were summed.

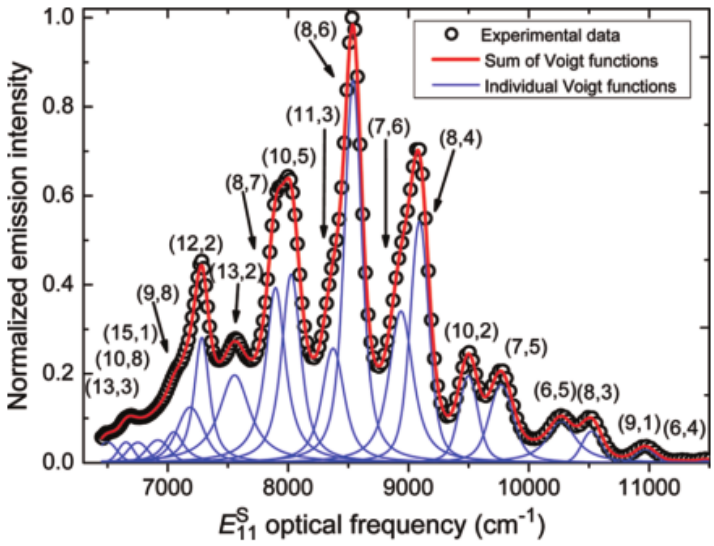

Figure 2.2 – Experimental vs computational spectra of emission at a excitation of 785nm. Voigt functions for different species of SWCNTs were calculated to show experimental spectra matches that of the computed spectra.[40]

It was found that the resulting simulated spectrum matched the experimental spectrum for a sample of SWCNTs excited at 785 nm.

Confirming that each (*n,m*) species of SWCNTs has its own emission profile that is observable even using off-resonance excitation wavelengths then allows for

development of experimental fluorescence methods that are optimized for interesting SWCNT studies.

2.1.2 *SWCNT specific issues in classic spectrofluorimetry*

The Classic method of fluorescence detection does have some undesirable issues for SWCNT studies. This is due mainly to an inner filter effect on the emitted light by other SWCNT in solution. The inner filter effect is an event that happens in the sample of SWCNTs. When one observes an absorption spectra of semiconducting SWCNTs, the two bandgaps have distinct regions of absorption, the S_{11} lying in the region of ~800 – 1900 nm and the S_{22} region lying between ~ 500 – 1200 nm. When conducting a fluorescence study, excitation is achieved over the S_{22} bandgap while emission is seen over the S_{11} bandgap. During excitation in fluorescence study the path of light brings the excitation light to the center of the sample and the emission then travels from the center of the sample to the wall of the sample and out. During the movement of the emitted light from the center of the sample till it is out of the sample a portion of the emitted light is reabsorbed by SWCNTs that are in solution but not excited by the excitation light. This event is confirmed though absorption spectra as it can be observed that there is absorption peaks in the region of the S_{11} bandgap where emission takes place. Since there is evidence that SWCNT fluorescence quantum yields are dependent on (*n,m*) structure and typically on the order of 0.1 – 10% in aqueous suspensions,[26] in order to accurately determine the (*n,m*) of a sample of SWCNTs the maximum amount of emission is needed to reach the detector.

A second issue with classic fluorescence studies is the source of excitation. The use of a tungsten lamp allows for a large array of wavelengths to be used as an excitation

source, but at the same time, the radiative power of the excitation light is non-uniform across a broad range of wavelengths, for instance from 300 to 900 nm. Additionally the excitation energy is typically spread over a larger surface area. These are unfavorable circumstances when studying SWCNTs because they affect the ability of the excitation source to adequately excite all the SWCNTs in solution.

2.2 Modifying the classic fluorimeter for SWCNTs

The first fluorescence instrument developed specifically for the spectrofluorimetric analysis of SWCNTs was by Rocha et al. from Rice University.[40] Their instrument was designed to replace the classic fluorimeter when studying SWCNTs. To optimize the new instrument for SWCNTs studies several changes were made to the classic fluorimeter mainly in the cases of path of light and excitation source (Figure 2.3).

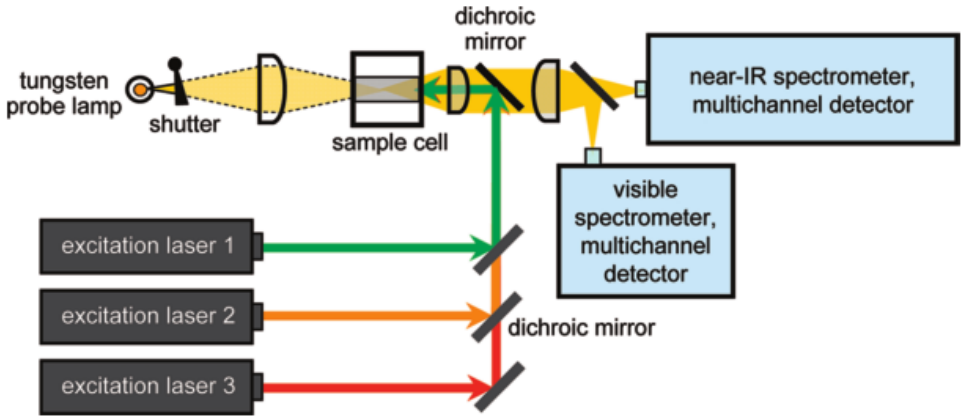

Figure 2.3 – Spectrofluorimetric analysis instrument designed at Rice University. Utilizes inline excitation and emission to reduce reabsorbance in SWCNTs and single wavelength light sources.[40]

First the path of light was altered. To reduce sample emission reabsorption concerns, the path of light was changed so that excitation light no longer had to travel to the center of the sample and the emission light would not have to travel the same distance through the sample. Similar to the design of a confocal microscope system, the excitation

light was brought in-line with the emitted light, to achieve a 0 degree angle, through the use of a dichroic mirror. Reflected excitation light is filtered out of the emitted light with the dichroic mirror. The dichroic mirror acts a long pass filter for the excited light, reflecting the visible excitation light onto the sample and allowing the emitted infrared light to pass through. A new focal point was achieved through the use of an aspheric lens. The aspheric lens not only moved the focal point of the excitation light closer to the surface of the sample but it also collimated the emitted light as it leaves the sample. This design minimizes the inner filter effect by reducing the path that the emitted light must travel through the sample. Emitted light then enters a near infrared spectrometer where the emission spectrum is formed.

The next change made by Rocha et al.[40] was to the excitation source. Knowing that the use of a tungsten lamp will have a reduced power at each of the wavelengths desired when isolated coupled with the low SWCNT emission quantum yields, the goal was to use a light source that had a higher power and did not require the light to be split. The solution to this issue was found in the use of lasers. Lasers offered a higher excitation power for each chosen wavelength and eliminate the need to use an excitation monochromator in the initial light path.

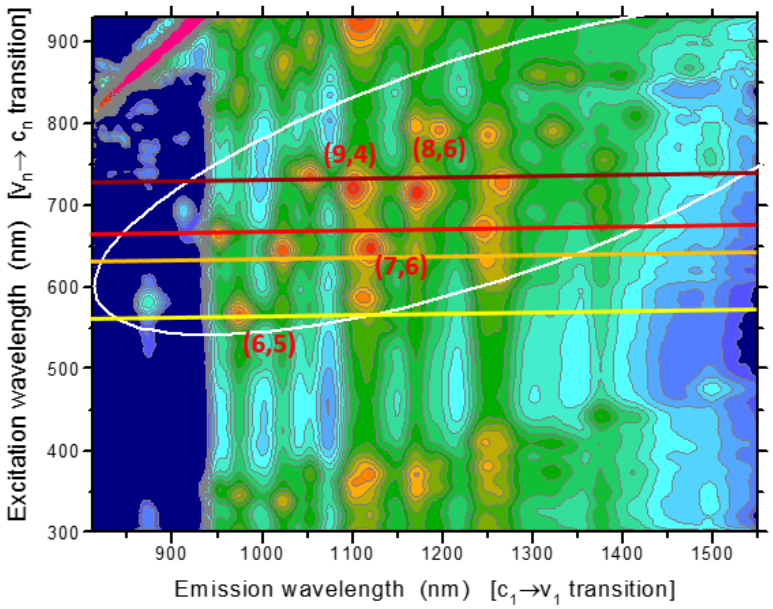

Figure 2.4 - 2D fluorescence illustrating the use of 4 lasers at 561, 640, 660, and 730 nm have the ability to excited >30 different species of SWCNTs.[6]

In order to use a laser as a source of excitation it must be able to excite a large array of (*n*,*m*) SWCNT types. The use of a laser can be confirmed by studying a 2D fluorescence spectral map of excitation vs. emission (EEM) for a sample of SWCNTs (Figure 2.4). Considering the EEM it was observed that for a cross-section at a given excitation wavelength overlapping of the emission of different (*n*,*m*) species occurs. It can be seen that a single laser has the ability to excite several different (*n*,*m*) in a sample (Figure 2.4). Several lasers can be used in series to excite the full dispersion of (*n*,*m*) types in a sample of SWCNTs. The use of 4 lasers in series has the ability to excite around 25 different (*n*,*m*) species.

This system design by Rocha et al.[40] allows for further modifications to the set of spectroscopic characterization methods to be added, such as Raman or UV-Vis-NIR absorption. With the laser excitation, an additional visible light detector (like a Si-CCD), and slight light path modifications, Raman spectroscopy can be observed. Absorbance can be taken for a sample of SWCNTs by adding a white light source and a visible light

detector. These modifications would allow a single instrument to be utilized for all optical spectroscopy for SWCNTs.

The specific reaction quenching rates for SWCNT (*n*,*m*) types resulting from either covalent or noncovalent interactions are still unknown and speculated to be very fast, possibly in the picosecond time scale. However, the initial system optimized for SWCNT fluorescence is not suitable for these real time reaction kinetic studies since it utilizes a detector only capable of millisecond timescale data acquisition. But, given that SWCNT emission in the near-infrared is weak due to low quantum yields, the changes made to the classic fluorimeter allow for the fluorescence spectrum of SWCNTs to be detected with higher sensitivity.

2.3 New instrument

To study the kinetics of functionalization of SWCNTs the J. Rocha, S. Bachilo, S. Ghosh et al. spectrometer was used as a basis for our setup as it deals with the issue of excitation source and the inner filter effect. Further changes to the Rocha et al. spectrometer are made so that we can detect the kinetics of a single (*n*,*m*) SWCNT in solution (Figure 2.5).

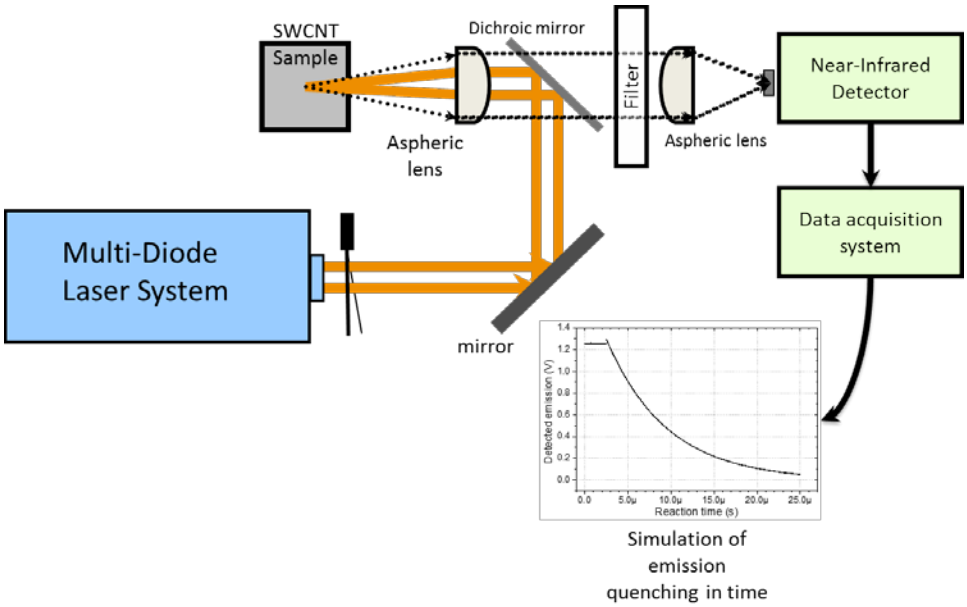

Figure 2.5 – Design of new instrument with modifications to the light source and path of light to allow for minimization of the inner filter effect and single wavelength excitation.

The first addition that is made is a series of bandpass filters in the path of the emitted light before it reaches the detector. Bandpass filters allow for the emission from a single (*n*,*m*) to be isolated from the emitted light from a polydispersed sample. Since the (6,5) SWCNT S_{11} bandgap is at 975 nm, kinetic studies on the (6,5) SWCNT will use a bandgap filter with a center wavelength of 980 nm and a full with half maximum (FWHM) of 10 nm. By changing the filter in front of the detector, studies can be done for different species of SWCNTs in a sample.

A sample holder was fabricated so that a 10 mm × 10 mm cuvette and a 10 mm × 2 mm cuvette can be held (Figure 2.6). The sample holder also houses the aspheric lens to the surface of the cuvette to allow for the focal length of the lens to be placed directly on the surface. The aspheric lens has a focal length of 4 mm and acts to collimate the emitted light as it leaves the sample holder. The first sample holder was constructed out of 1/4" aluminum and drilled with 8-32 tapped holes to allow for the sample holder to be deconstructed and rearranged for future adaptations of the instrument. Two of the sides of

the sample holder have windows to mount the aspheric lens. One window was drilled with a size M hole and tapped with a M8-0.5 tap and the other was drilled with a size O hole and tapped with a M9-0.5 tap.

Figure 2.6 – On the right is sample holder 1 which was constructed with the ability to be broken down and connected by screws and on the left is sample holder 2 is a permanent holder that is constructed with epoxy.

Problems with the first sample mount arose in the instability of the side walls. Due to the placement of the set screws to hold the mount together to allow for the maximum space for the windows the sample holder was loose due to misaligning parts and shallow tapped holes. In addition to the stability issues the windows were not aligned to future adaptations of the instrument. To correct these issues a second sample holder was constructed. The stability issue was addressed with fast setting epoxy to hold the sample holder together, although this makes it so that the sample holder cannot be rearranged. The second sample holder also featured two windows in alignment to allow for the pass through of light should adsorption be added to the instrument in the future.

Fabrication of a mirror mount was vital for the ability of the mirror to be in close proximity to the sample holder while still acting as a long pass filter for the emitted light

(Figure 2.7). The first mirror mount was designed to hold the mirror between two pieces of aluminum. The first piece of aluminum is ¼" aluminum with a 1/8" channel milled to hold the mirror from sliding left to right will allowing the mirror to slide into place from the top. The second piece of aluminum is 1/16" and holds the mirror from falling out of the first piece of aluminum. Problems came when milling in the 1/8in channel. With the first piece being only ¼" there was little room to mill the channel to hold the mirror and drill holes so the mount can sit on an optical post.

Figure 2.7 – Mirror mount 1 which held the mirror between two pieces of aluminum, Mirror mount 2 which cut and mounted mirror onto an optical post with epoxy, Mirror mount 3 which used a larger mirror and reduced the space between mirror and sample holder.

A second mirror mount was fabricated by cutting the mirror to a ¼" x ¼" square. This was then mounted into a block of aluminum with a 1/8" groove to allow for the mirror to be mounted with fast setting epoxy. This mirror mount was insufficient because the small piece of aluminum that hung in front of the mirror inhibited the mirror from coming close to the sample holder. The second mount also allowed for excitation light to pass around the mirror. A third mirror mount was fabricated in a similar fashion to the

second mirror mount with no overhanging aluminum in front of the mirror and a larger ½" x 1" mirror to minimize the amount of light passing over and around the mirror.

Further modification to the instrumental setup comes in the form of changes made to the detector and data acquisition setup. In the Rice setup[40] emission is dispersed by a near-IR spectrometer with multi-channels. This setup is optimal for the determination of (*n*,*m*) in a sample but not ideal for kinetic studies because it slows down the instrument and does not capture the most amount of emitted light as possible. Modification to the detector and data acquisition starts with the single element detector. The use of fast rising detectors is needed for studying SWCNT kinetics because the reactions happen on the sub-millisecond time scale so a detector needs to be fast enough to be able to catch the small fast changes in the intensity of light. To do this, two different types of detectors will be used: one based on silicon with a detection range of 400 – 1100 nm, and the other based on indium gallium arsenide (InGaAs) with a detection range between 800 – 1700 nm. Two different Si detectors, with rise times of 14 and 43 ns, will be tested. The silicon detectors are ideal for studies with the (6,5) SWCNT type because the detectors peak detection efficiency is at ~1000 nm. Along with the silicon detectors, 3 different InGaAs detectors with rise times of 10, 6, and <1 ns are to be used. The InGaAs detectors will allow for studies to be conducted of all typical semiconducting species of SWCNTs.[9] Due to the fast rise times of the InGaAs detectors, kinetic studies occurring as fast as the picosecond time scale may be observed.

When trying to collect fast real-time kinetics of SWCNTs, a fast data acquisition system is needed in relation to the fast detector. A fast data acquisition system will allow the instrument to measure the intensity of the fluorescence at a sample rate fast enough to

capture the quenching of the SWCNT fluorescence as the SWCNT is functionalized. The detector chosen to the modification to a kinetic analysis instrument was an Agilent U1071A Acqiris. The Agilent U1071A Acqiris has a sampling rate of up to 2 GS/s, and can be programed using LabVIEW.

LabVIEW is a graphical programing software environment offered by National Instruments that allows for custom program to be written for different application. Through the LabVIEW software a virtual instrument (VI) was setup to allow for test parameters to be set for each trial (Appendix A1). In LabVIEW, parameters such as sample rate, sample size, trigger slope, trigger level, and trigger delay can all be modified so that each trail is optimized. Incorporated into the LabVIEW VI for the data acquisition are the controls for the four different lasers that will be utilized. Whenever using lasers safety is the utmost concern, so failsafes were written into the program so that users have full control of the laser. The first of the controls for safety are a two switch activation system where each laser has an enable and start switch. The enable switch powers the laser without emission. This allows for the laser system to stabilize before light is emitted. Only when the laser is enabled will the start switch cause activation of the excitation light. The laser system is on a for loop outside of the data acquisition VI that is not limited by a number of iterations, this means that after the VI is done with the data acquisition the controls for the laser are still active and the laser can safely be turned off. (Figure 2.8)

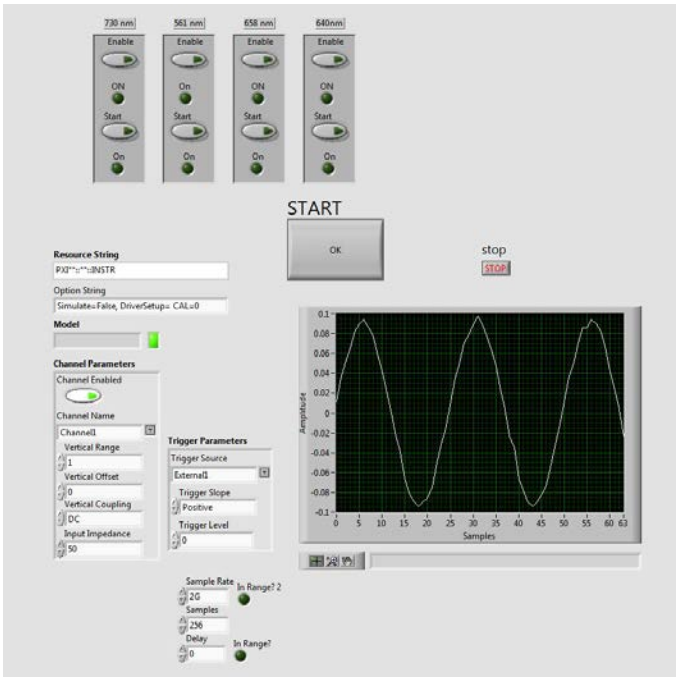

Figure 2.8 – Front panel of LabVIEW software for fluorimeter.

Lasers were purchased from Toptica Photonics in a multi laser engine (iChrome MLE) that emits all four lasers from a single fiber optic output with no overlapping of wavelengths. Wavelengths chosen were 561, 640, 658 and 730 nm. These wavelengths will provide the widest array of SWCNTs fluorescence. Inital tests was conducted using the561 nm laser. The 561 nm laser excites the (6,5) SWCNT that has a E_{22} bandgap of 566 nm that comprises 40 % of the SWCNT species in the sample.

Initial tests of the new system were completed with the use of laser dyes LDS 950 and IR 430 purchased from Exciton. LDS 950 has an absorbance range of 464 to 804 nm with an absorbance max of 612 nm and an emission range of 928 to 1084 nm with a emission max of 980 nm. IR 143 has an absorbance range of 488 nm to 915 nm with an absorbance max of 840 nm and an emission range of 913 nm to 1020 nm with an emission max of 960 nm. With these dyes we are able to monitor the amount of emission from a control to show that the path of light from excitation to emission was correct, and

in addition, we verified that the LabVIEW VI is accurately controlling the laser and the data acquisition card to monitor the dye fluorescence emission in real-time.

Initial runs on of the system showed a poor signal to noise ratio. When building the array of data points, the signal is lost in the noise and measures need to be taken to adjust for such a problem.

Methods for signal to noise correction can come in two forms; a software correction or a hardware correction. Software corrections are most commonly done through the averaging of several data points. For example, several scans are run and the average of each data point is taken, and then the resulting average spectrum is reported. Software correction can also be achieved through a Fourier Transform that separates the real and imaginary functions of a time oscillation to produce a data spectrum, this too is best done after several scans to decrease noise. Because measurements of SWCNT reaction kinetics will be a single scan method software corrections are not applicable.

One form of hardware correction comes in the form of operational amplifiers. Such electronic units have the ability to reduce the amount of noise by increasing the strength of the signal while keeping noise constant. Another form of improvement to the signal to noise comes in the form of a thermoelectrically cooled detector. Both of these methods were looked at for this system, so we purchased from Thorlabs an InGaAs Amplified Photodetector with Thermoelectric Cooler (PDA10DT). This detector has a bandwidth switch over the ranges 500 Hz – 1 MHz and a gain switch that ranges from 0 – 70 db. The thermoelectric cooler can hold the temperature to -10 $^{\circ}$C. Since the detector operates in the near-infrared region of the electromagnetic spectrum, radiative temperatures from the ambient environment and sometimes even electronics can induce

significantly detectable ‘dark’ noise. By cooling the detector, this ‘dark’ noise is minimized. The use of the gain will allow for amplification of the signal but has an adverse effect in that it slows down the speed of the detector. The use of the gain will allow for a stronger reading but will not allow for the possible picosecond kinetics to be detected.

Using the thermoelectrically cooled InGaAs amplified photodetector, fluorescence was observed in the LDS 950 laser dye in a 90° configuration using the 640 nm laser. In the set up for the 90° configuration the dichroic mirror and aspheric lens were removed to attempt to isolate the loss of the emitted light. When the mirror and lens are reintroduced into the system and the configuration is returned to the inline setup, then the emission is lost again.

Two possible problems that could result in the loss of emission lie in the angle of the dichroic mirror and the possibility of the aspheric lens being mounted on an angle in the sample holder. If the mirror is not in a position that will allow the excitation light to enter the sample holder perpendicular to the sample holder the focal point through the aspheric lens will be shifted to the side, this will minimize the amount of emission that is collimated as the light leaves the sample holder because the collimated light will be comprised mainly of divergent emission and not the emission from the focal spot. One way that this issue can be corrected is to place two focusing mirrors in the path of excitation. Focusing mirrors will allow for small corrections to be made to the path of light so ensure that the path of excitation light enters perpendicular to the sample holder (Figure 2.9).

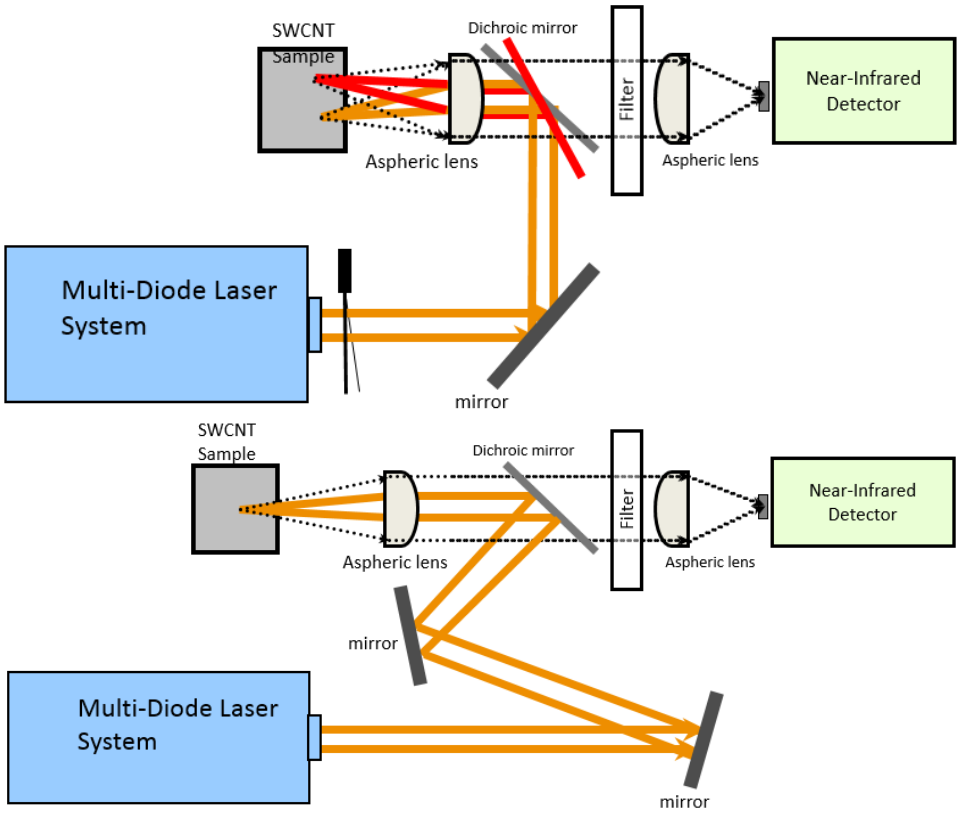

Figure 2.9– (top) Effects that a mirror has on path of light illustrating how the focal point can change with the mirror (bottom) Focusing lens can correct for improper placement of dichroic mirror.

If the aspheric lens is not properly mounted inside the sample holder it will not only move the focal point out of the window but it will also change the path of emission so that it is no longer 180° to the excitation path (Figure 2.10).The way to correct for this issue is to either reconstruct the sample holder and tap new holes ensure the aspheric lens are mounted straight into the sample holder. The other possible solution would be to have the sample holder constructed using a CAD system that will ensure proper construction.

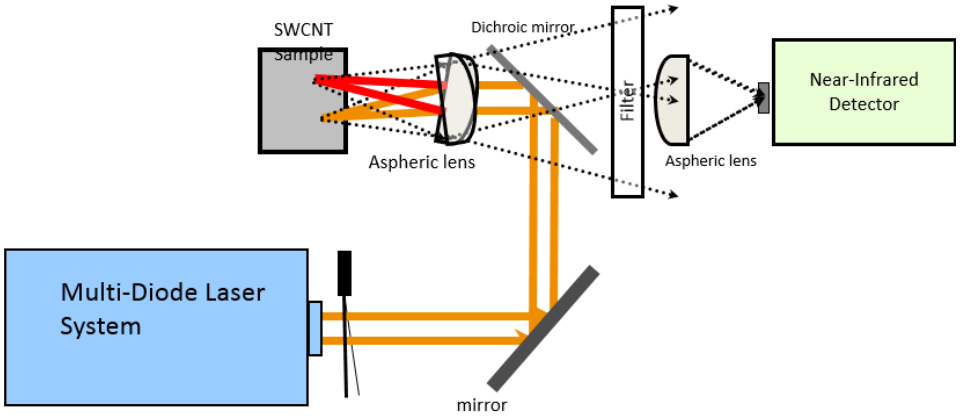

Figure 2.10 – Illustration of how a improper placed aspheric lens can alter the focal point of the emission.

Finally, the addition of a focusing lens in the path of emission after the bandgap filter will allow for the more emission to be focused onto the detector. A focusing lens will allow for collection of not only the collimated light but also the divergent light that escapes from the collimation. The detector only has a 0.5 mm active window and the use of a focusing lens will allow for the highest efficiency of the system.

The modifications to the spectrofluorimeter built by Rocha et al. will allow for fast kinetic of SWCNT reactions to be detected. Through the use of the Toptica multi laser engine and fast data acquisition the kinetic of SWCNT reaction will provide information that will allow for better understanding of the interactions that take place in SWCNT separations, and investigation into possible integration of SWCNTs into applications. LabVIEW provided the ability to customize the programing of the instrument to meet the needs of the instrument. Fabrication of a mirror mount and sample holder with mounted aspheric lens allows for an inline excitation/emission setup to minimize the absorbance of emitted light.

Although issues arose in the completion of the new instrument, there is promise for a future direction with the solutions previously mentioned. Once fully operational this instrument will prove to be a valuable research tool.

CHAPTER 3 – UNDERSTANDING OF INTERACTIONS LEADING TO SEPARATIONS OF METALLIC AND SEMICONDUCTINGSWCNT DISPERSIONS VIA STEP-GRADIENT GEL CHROMATOGRAPHY

3.1 Introduction

Single-walled carbon nanotubes (SWCNTs) are nanostructure of carbon that have unique physical and electrical properties making them a topic of interest in many different fields of research ranging from alternative energy, to electrical wires and can be used for their textile strength.[8, 11] The use of SWCNTs in such applications depends on the ability to isolate different (*n*,*m*) structural species from a mixed sample to fully exploit their unique characteristics. SWCNT characteristics depend on variations in the diameter (*d*) and chiral angle (θ) of the structure, enumerated by the (*n*,*m*) designation (See previous discussion in Ch. 1, sec. 2), that allows for different mixing or overlapping of the π-orbitals. These variations result in, among other things, SWCNTs with either metallic or semiconducting properties.[5] SWCNT production, be it either laser pulse, arc discharge, or chemical deposition such as HiPco or CoMoCAT™, results in a dispersion of different species, 1/3 of which are metallic and 2/3 are semiconducting.[8] Again, in order to apply SWCNTs to a wide array of electrical uses the *(n,m)* semiconducting SWCNTs must be separated so that each SWCNT with specific electrical properties (in this case, bandgap energy) can be selected for a given application. There is a need to find a method of separation that has the ability to isolate a single species of SWCNTs from a mixed sample that is simple in both its execution and confirmation of results, as to lead itself to be scaled to an industrial application.

Current methods of separation, such as density gradient ultracentrifugation or gel electrophoresis, although proven for their ability to separate SWCNTs into different

chiralities have fallen short in their ability to be scaled up to industrial quantities.[41, 42] In other previous work by Hirano et al. and Tvrdy et al., it has been shown that a heterogeneous sample of SWCNTs can be separated to yield a single (*n*,*m*)-type enriched sample through gel chromatography using Sephacryl-S200 agarose (or a similarly structured allyl dextran) gel.[43, 44] In each study, small amounts of gel are used and several different columns are run in order to isolate all of the different (*n*,*m*) species in a sample. These methods as described, though effective, do not lend themselves to being scaled to an industrial level due to being both time and labor intensive, also including high centrifugation forces (>100,000×*g*) and sonication powers (>15 W·mL/g).

In the work done by Strano's group at M.I.T., a proposed kinetic model states that different species of SWCNTs have different affinities to the secondary amines on the Sephacryl gel.[44] Sephacryl is an allyl dextran polymer that is cross-linked with N, N'-methylene bisacrylamide that is traditionally used in biochemistry as a size exclusion gel for the purification of proteins and polysaccharides.[45] Smaller diameter SWCNTs have a higher affinity to the gel than the larger SWCNTs. When a sample is passed through a 1.6 mL column, the small diameter SWCNTs with the high affinity bind to the gel and the rest of the species pass through the gel. When the concentration of the SDS eluent solution is increased, the small diameter SWCNTs were released from the gel and collected. This was repeated 30 times with the next highest affinity being bound on the next successive column each time.

Silvera-Batista et al. sought to determine the interaction that drives the adsorption of SWCNT to Sephacryl-s200.[46] Silvera-Batista et al. determined that the affinity of the SWCNT to the gel depends on the amount of SDS that is bound to the surface of the

nanotube. If the separation is size- exclusion driven as the gel is generally used there would be no need to change the mobile phase to elute all the SWCNT from the column. What Silvera-Batista et al. found was to remove the bound SWCNTs, the concentration of the SDS needs to be increased, for instance from 2 wt% to 5 wt% (69 mM and 173 mM, respectively), to break the interaction between the SWCNT and the gel.[46]

Further work from Jain et al. (Strano's group) recently confirmed that the interaction bonding energy of the semiconducting SWCNTs and the gel was a result of: 1) the van der Waals forces that bond a SWCNT to the gel, 2) the electrostatic repulsion that is a result of the anionic surfactant and the secondary amines on the Sephacryl gel, and 3) the hard-surface repulsion of the SWCNT and the gel.[47] Due to incomplete wrapping of the SDS around the SWCNT surface, the different SWCNTs will have a different affinity to the gel depending on the diameter of the SWCNT.[48, 49] To release the SWCNTs from the gel, an increase in SDS will increase the repulsion between the SDS/SWCNT micelles and the secondary amines, thus releasing them.

With this information, we devised a method to allow for the separation of the different species in a single column. Knowing that the SWCNTs are bond to the gel, the first goal is to get as many of the sc-SWCNTs in a sample to bind to the column as possible. This will allow for a single column to be used for the separation of semiconducting *(n,m)* using Sephacryl gel. In previous work, the goal was to only have one species of SWCNT bond to the gel at a time, so small quantities of Sephacryl were used. Adsorption of SWCNTs to the gel is a result of an interaction between the secondary amines on the N, N'-methylene bisacrylamide and the sections of the SWCNTs that are not covered in surfactant. To allow for the greatest number of

SWCNTs to bond there needs to be more bonding sites open allowing the maximum amount of sc-SWCNTs to adsorb to the column. In other studies, a small column of only 1.6 mL of gel are used limiting the amount of SWCNTs that adsorb. To allow for the maximum amount of SWCNT retention a longer column of 30 cm was used by adding 6 mL of gel to the column.

With the most possible sc-SWCNTs bound, next was to remove the SWCNTs one species at a time. It has been shown that in order to remove the bound SWCNTs from the column the surfactant must be changed to one with a higher affinity to the SWCNTs. Sodium cholate is commonly used for this purpose. In the work by Tvrdy et al. it was shown that to remove the bound SWCNTs from the column an increase in the surfactant concentration, to say 5 wt% SDS, has the ability to release the SWCNTs so that the surfactant does not have to be changed.[44] It was postulated that the concentration of SDS needed to elute the SWCNTs is related to the affinity of the SWCNT to the gel. So larger diameter SWCNTs will elute with a low concentration of SDS while smaller diameter SWCNTs will require a stronger concentration of SDS to elute the SWCNTs.

A new method described here demonstrates that varying the concentration of the mobile phase in a gel-based chromatography column will achieve similar results to those previously found in published literature using more elaborate techniques, such as multicolumn methods needing ultrasonication and ultracentrifugation. This method will also help us understand the differences between the interactions SDS and other surfactants for the purpose of SWCNT separations.

3.2 Experimental Methods

3.2.1 Sample Preparation

10 mg of CoMoCAT SWCNTs (SWeNT SG-65i) was placed in 20 ml of 0.5 wt% SDS (Sigma-Aldrich) and sonicated for 5 hr (~12 W) using a Cole Palmer microtip bell sonicator (1/8” tip). During sonication the sample was placed in a water cooled bath (~ 10 ºC) to maintain constant temperature. The sample was then centrifuged in a Hettich Zentrifugen Mikro 200 for 90 min at 18,000 rpm (31,000 × *g*) to remove any impurities and bundles of unseparated SWCNTs. The top 80% of the samples was decanted from each centrifuge vial and kept while the resulting pellet discarded.

3.2.2 Chromatography

Gel-based chromatography was performed in a 12 mL disposable syringe, 72 mm in length, and a diameter of 16 mm. 6 mL of Sephacryl-S200 (Sigma-Aldrich) was added to the syringe resulting in a column 30 mm in length. 18 mL of 27 mM SDS was passed through the gel to remove the ethanol that is present in the commercial as-received gel. Each SWCNT sample was sonicated for an additional 10 min prior to addition to the column to prevent aggregation before chromatography. 1 mL of sample was added to the column and allowed to adsorb to the gel before any surfactant gradient was applied. After the sample has adsorbed to the gel, a step gradient from 27–247 mM SDS in 10 mM steps was applied by the addition of 6 mL of solution to the column and collecting the fraction in 6 mL increments before the next SDS solution was added. Unregulated air pressure was applied to the column that resulted in a flow rate of 2 mL/min.

3.2.3 *Absorption spectroscopy*

Absorption spectra were taken for all fractions using a Perkin-Elmer Lambda 25 spectrophotometer running UV Winlab software. Spectra were taken at 0.5 nm intervals for a range of 350 – 1100 nm at a speed of 960 nm/min. Data was analyzed using Origin data processing software to create a contour map of the absorbance vs surfactant concentration. All spectra were normalized in between the S_{11} and S_{22} bandgaps at 780 nm.

3.3 Results and Discussion

3.3.1 Theory behind separation

For this study, CoMoCAT SWCNTs were selected because of the ability of the CoMoCAT process to produce a sample with a small diameter range and the ability to produce a high concentration of (6,5) SWCNTs. Data shared by the manufacturer indicates the (6,5) to be ~40% of the overall sample.[21]

Sodium dodecyl sulfate (SDS) is responsible for the creation of micelles around individual SWCNTs during sonication, an effort that interferes with the attractive forces in between SWCNTs originally produced in bundles. The hydrophobic tail of the surfactant is what interacts with the SWCNT. This is due to the fact that the SWCNT is a carbonaceous material and is hydrophobic in nature. Previous work done by, Silvera-Batista et al. has shown that the amount of SDS residing on the surface of the SWCNT is dependent on the diameter of the SWCNT and not the chiral angle,[50] larger diameter SWCNTs have more SDS on the surface of the tube than smaller diameter tubes. The correlation between the amount of SDS on the surface of the nanotube and the diameter of the nanotube results in a change in affinity of the semiconducting SWCNTs to the

Sephacryl gel. Additionally, the presence of too much SDS leads to minimal interactions for the sc-SWCNTs to the gel media, while too little SDS results in irreversible binding. This is important when attempting to separate a heterogeneous sample into isolated samples of specific SWCNT (*n,m*) types. By increasing the concentration of SDS in the mobile phase, the adsorbed SWCNTs are released from the gel by increasing the amount of repulsion the surfactant applies between the SWCNT and the Sephacryl gel. When the mobile phase is applied as a concentration gradient the different affinities of the semiconducting SWCNTs can be exploited producing *(n,m)* enriched fractions.

3.3.2 Retention of semiconducting SWCNTs to Sephacryl gel

First separation of metallic and semiconducting SWCNTs was done so that we can assure that the greatest amount of sc-SWCNTs adsorbed to the column (Figure 3.1), thus allowing for better separation of the semiconducting species as they adsorb to the gel. Smaller diameter SWCNTs with higher affinity will adsorb more strongly to the column while large diameter SWCNTs will adsorb weakly to the column, thus creating a gradient in the column from smaller diameter SWCNT to larger diameter SWCNTs. To achieve the maximum amount of SWCNTs bound to the column three different surfactants were tested to suspend the SWCNTs in solution. SDS was able to elute the metallic SWCNTs as well as any unbound semiconducting SWCNTs with 69 mM SDS while leaving the majority of the semiconducting SWCNTs bound to the column. The sc-SWCNTs were eluted with 173 mM SDS. SWCNTs suspended in SDBS showed no affinity to the column with all of the SWCNTs eluting in 28 mM SDBS. When the SWCNTs are suspended in AOT and separated by gel chromatography, the SWCNTs that eluted at a concentration of 3 mM AOT were identical to the SWCNTs that eluted with

33 mM AOT, indicating that both metallic and semiconducting SWCNTs were eluted in each fraction. This will inhibit the ability to produce a *(n,m)* enriched sample as the *(n,m)* of metallic SWCNTs cannot be determined through column chromatography.

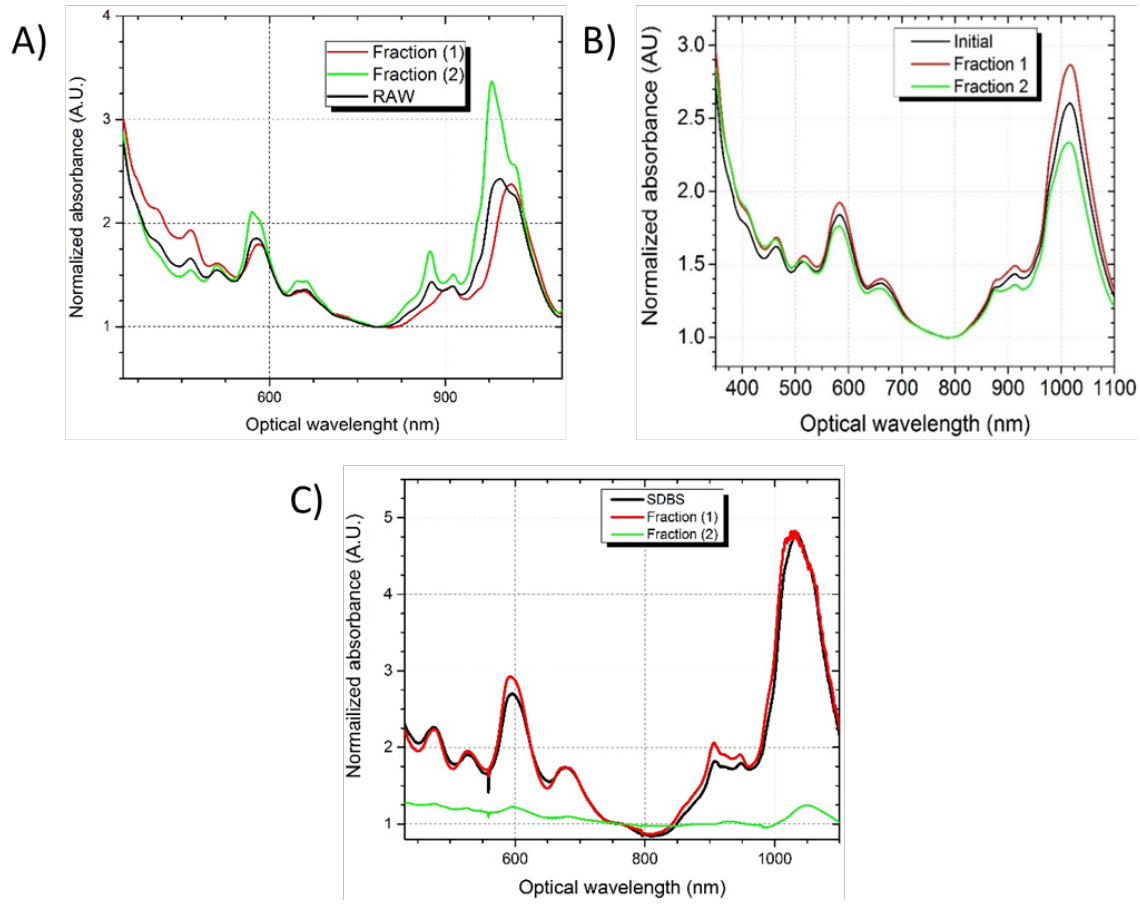

Figure 3.1 – Absorbance data of separation of metallic enriched fraction from semiconducting enriched fraction SWCNTs. Data was normalized at 780 nm as there is no overlapping of E_{22} and E_{11} energy gaps. A) Separation by SDS B) Separation by AOT C) Separation by SDBS

When applying a gradient of the eluting surfactant to a column with semiconducting SWCNTs adsorbed to the gel it was observed that the large diameter tubes elute from the column before the smaller diameter tubes. This is most likely a result of the moderated interactions between the secondary amines on the Sephacryl gel and the SWCNTs with large amounts of SDS on the surface compared to SWCNTs with small

amounts of SDS on the surface. To release the SWCNT from the gel a concentration of SDS must be used that will increase the repulsion of the SWCNT and the gel. Large diameter SWCNTs have more SDS on the surface due to the fact that the larger diameter allows for more conformational arrangements of the SDS on the SWCNT. On larger diameter SWCNTs the SDS can lay parallel or anti-parallel to the SWCNT. SDS on smaller diameter SWCNTs lay in a parallel formation. Larger diameter tubes have less strain on the SDS when wrapping around the SWCNT anti-parallel resulting in more aggregation of gel to the surface.[49, 51]

Enrichment of a single species can be archived by using a gradient as will be discussed in section 3.3.2 with SDS as the mobile phase. To enrich a *(n,m)* species one would use a concentration of surfactant directly below the concentration that will release the SWCNT of interest, this will elute all of the SWCNTs not of interest into a single fraction. The next step in the gradient will elute the SWCNT of interest. When this method was applied to elute a fraction enriched in (6,5), 127 mM SDS was used to elute the *(n,m)* not of interest and 137 mM was used to elute a fraction enriched in (6,5).

3.3.3 *Separation by SDS gradient*

Metallic SWCNTs, which have no affinity to the Sephacryl gel, can be seen in the first two fractions as they elute with no changes to the surfactant. Along with the enriched metallic peaks, absorbance can be seen in the regions of the S_{11} and S_{22} of the spectra. This is due to the large broadening of the absorbance peaks that result from an overlap of peaks. We believe this is a result of unbound tubes that have not adsorbed to the surface of the gel along with small bundles of SWCNTs that remained in solution after centrifugation.

When monitoring the major peaks of the elute from the column we can see that the first SWCNTs to elute from the column are a mixture of the (7,5) and the (7,6) eluting from the column after the metallic SWCNTs from a range of 27 mM to 47mM. (Figure 3.2) Next to elute from the column was the (7,3) eluting in only a single fraction at a concentration of 97 mM. After the (7,3), the (6,5) elutes in a range of 107 – 200 mM with a maximum amount at 137 mM. The peak for (6,5) is observed with an absorbance maximum at 980 nm result in the highest intensity of peaks as it is the most abundant species of SWCNTs in the column with 40% of the initial material being (6,5). We see one more main peak elute from the column from a range of 127 – 157 mM from (6,4) SWCNT. After a concentration of 187 mM of SDS is reached, no more significant peaks were observed. As no separation method has been able to produce a sample of a single *(n,m)* SWCNT species, no absorption extinction coefficients have been reported. With a lack of extinction coefficients we have no understanding of the role concentration plays on the intensity of the absorbance peak. Upon inspection of the column after the completion of the gradient, several SWCNTs remain bound to the column. These are believed to be irreversibly bound tubes and impurities that remained in solution after centrifugation. At this point we do not have an understanding of what species of SWCNT become irreversibly bound to the column.

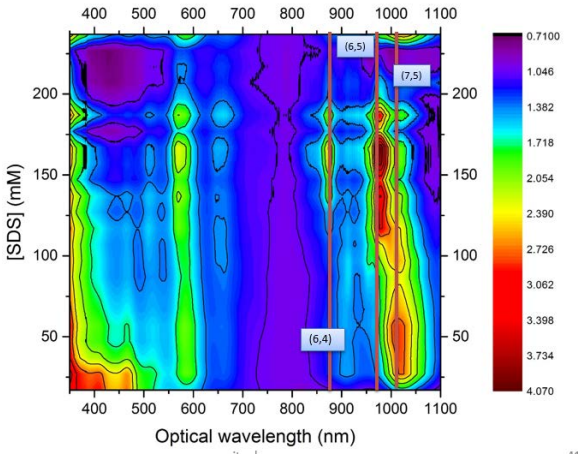

Figure 3.2 – Concentration of SDS vs Absorbance from SDS gradient showing separation of different *(n,m)* as the concentration of SDS increases. Separation can been seen between different *(n,m)* by diameter with smaller diameter SWCNTs eluting first, followed by larger diameter SWCNTs.

To demonstrate the ability to isolate a single species of SWCNTs by using a step gradient, an isolation of the (6,5) was done. First a concentration of 27 mM SDS was used to remove all of the metallic SWCNTs and unbound semiconducting SWCNTs from the sample. To remove all of the SWCNTS with diameters larger than (6,5), a concentration of 127 mM SDS was used. To accurately recover the (6,5) species from the column, a concentration of 137 mM SDS was used. This was selected because our data (Figure 3.3) indicates that a neighboring peak due to the (6,4) SWCNT type has enhanced absorbance following elution with an SDS concentration of 147 mM.

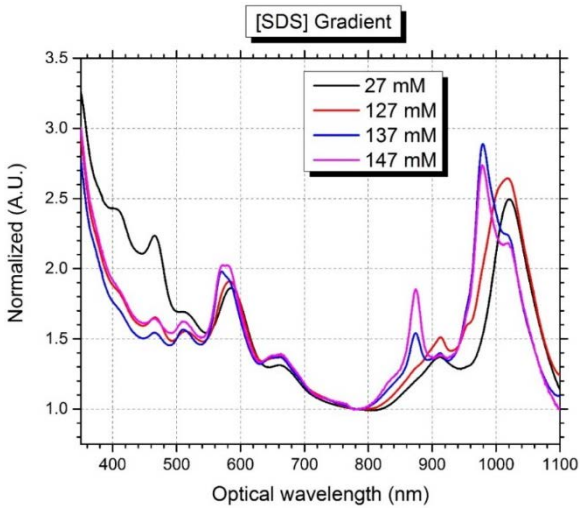

Figure 3.3 – Absorption spectra of fractions eluted with 27 mM, 127 mM, 137 mM, and 147 mM showing increased abundance of different (*n,m*).

Grouping of *(n,m)* species was observed in each step of the gradient, grouping is a result of SWCNTs with similar affinity eluting in the SDS concentrations between the gradient steps. This is prevalent when observing the absorbance spectra of the eluted SWCNTs at concentrations of 137 mM and 147 mM. We can see that the (6,4) peak overlaps with the eluting concentration with the (6,5).

3.3.4 Peak analysis of SDS fractions

Because of the small diameter range of SWCNTs in the sample many of the absorbance peaks overlap making separation analysis more difficult. In order to analyze the relative abundance of different species in the overlapping peaks, a method of peak fitting was utilized. This method is adequate at providing relative abundance on relation to the overall peak area of the overlapping peaks.

Assuming that all of the SWCNT (*n,m*) types have a similar extinction coefficient, integration of the peaks can show relative abundance of each species in a sample as the gradient moves from low concentration of SDS to a higher concentration of SDS. What was observed was the peaks of larger diameter SWCNTs are first prevalent with low

concentrations of SDS while smaller diameter SWCNTs are not present until higher concentrations of SDS.

Peak analysis was conducted by fitting Voigt functions (Equation 3.1) to the different species of SWCNTs. Using information provided in the SWCNT datasheet by the producer, SWeNT (SG65i Lot# SG65i-L39), and prior published literature[9], the abundant species are; (10,2), (8,1), (7,5), (7,3), (6,5), (8,3), (9,1), (6,4), and (5,4).

$$y = y_0 + A \cdot \frac{2\ln 2}{\pi^{3/2}} \frac{w_L}{w_G^2} \cdot \int_{-\infty}^{\infty} \frac{e^{-t^2}}{\left(\sqrt{\ln 2}\,\frac{w_L}{w_G}\right)^2 + \left(\sqrt{4\ln 2}\,\frac{x - x_c}{w_G} - t\right)^2} dt \tag{3.1}$$

$$y = y_0 + \frac{Ae^{\frac{-4\ln(2)(x-x_c)^2}{w^2}}}{w\sqrt{\frac{\pi}{4\ln(2)}}} \tag{3.2}$$

$$y = y_0 + \frac{2A}{\pi} \frac{w}{4(x - x_c)^2 + w^2} \tag{3.3}$$

Voigt functions are a combination of Gaussian (Eqn 3.2) and Lorentzian (Eqn 3.3). The Lorentzian portion represents the natural line broadening due to excitation lifetimes while the Gaussian lineshape arises from inhomogeneous broadening resulting from the sample being a mixture with different (*n*,*m*) species and differing extents of SWCNT defects or imperfections.[52]

As with most simulated peak fittings, bounds were put in place so that results did not violate photophysical properties. The area, *A*, was set to be greater than or equal to zero so that no peak would have a negative area, the width of the Gaussian (w_G) and Lorentzian (w_L) components of the Voigt function were limited to 250 cm^{-1} so that it would not result in overly wide peaks that are uncharacteristic for SWCNTs.[22, 38, 53] The

primary peak center positions, x_c, were set initially at the E_{11} transition frequencies (in cm^{-1}) and allowed to move ± 10 cm^{-1} for the set of SWCNT (*n*,*m*) species potentially present and observable in the range of 9100 cm^{-1} to 12,500 cm^{-1} (1100 – 800 nm) (Figure 3.4).

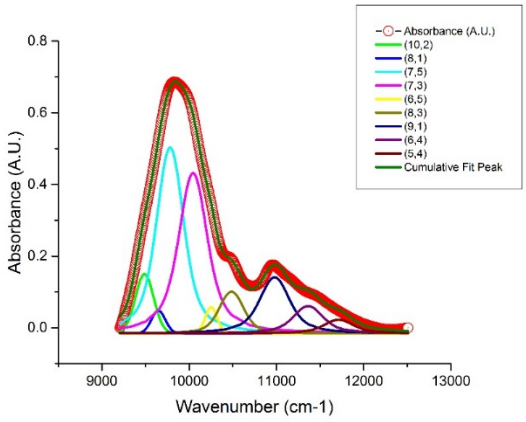

Figure 3.4 – Representative absorbance spectrum with simulated spectral data for fractions eluted with 127 mM SDS.

Results from the peak fitting indicate that the (7,5) (Figure 3.5)SWCNT elutes in the first fraction with the 127 mM SDS resulting in 32.1 ± 0.1% abundance. When concentration of SDS was increased to 137 mM the (7,5) area was decreased to 18.5 ± 1.6% and dropped further to 17.1 ± 1.2% when the SDS was increased again to 147 mM. This trend can be seen with other large diameter SWCNTs in the sample, the (10,2) decreased from 5.1 ± 0.4% to 2.5 ± 0.7% and the (9,1) and (8,1) dropped from 11.5 ± 0.1% to 6.3 ± 0.1% and 3.4 ± 1.1% to 0.3 ± 0.1%, respectively . Errors are based off the standard deviation of 4 peak fittings on a single spectral dataset.

Peak fitting indicates that the 137 mM SDS solution eluted more of the (6,5) SWCNT than the 127 mM solution, as the abundance changed from 1.4 ± 0.1% to 23.3 ± 1.2 % and then decrease to 20.9 ± 0.8% when the 147 mM SDS was used. Peak fitting

shows that the (6,4) elutes better with the 147 mM the abundance is 18.4 ± 0.1%, it was previously 5.6 ± 0.1% and 12.3 ± 0.2% in the 127 mM and 137 mM respectively and the column as the ability to produce enriched samples even when the eluting of two different *(n,m)* are close in eluting concentrations .

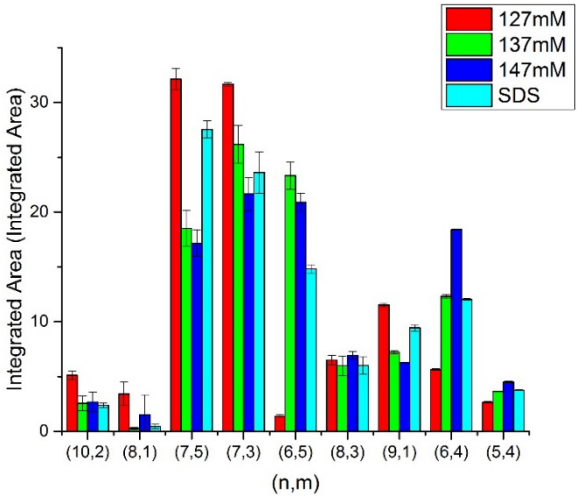

Figure 3.5 – Summary of peak fitting of the fractions with SDS gradient

3.3.5 Separation by SDBS gradient

We compared the effects of the mobile phase by using a different solvent to elute the SWCNTs. The use of a different surfactant provides the potential to reduce the overall cost of the separation as well as improve the recovery of SWCNTs that might have remained adsorbed to the gel with SDS as the eluent. Sodium dodecylbenzenesulfonate (SDBS) was chosen because it has the same chemical structure as SDS with the addition of a benzene ring. Also earlier literature states that SDBS has the highest ability to separate the SWCNTs from the bundles at low concentrations.[22]

A gradient of SDBS (Figure 3.6) was created from 0.25 wt% to 6 wt% in intervals of 0.25 wt%. The 0.5 mg/mL sample in 0.5 wt% SDS was used to observe the competition between the SDS and the SDBS. 0.5 wt% SDS was used first to elute the

metallic SWCNTs and then the gradient of SDBS was applied to elute the semiconducting SWCNTs.

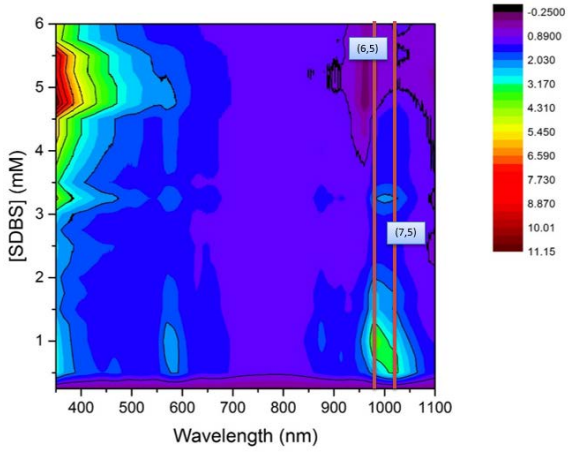

Figure 3.6 – Illustration of absorbance data for SDBS based gradient elution.

It was observed that most of the SWCNTs that were added to the column remained on the column after the gradient elution was finished. This was confirmed through absorbance data of each fraction of the gradient that showed small amounts of SWCNTs in each fraction with no distinction between different SWCNT species.

3.3.6 Separation by AOT gradient

The third surfactant tested was dioctyl sodium sulfosuccinate (AOT) (Figure 3.7). AOT is a surfactant that is most commonly used in reverse micelle encapsulation. This means that instead of encapsulating the hydrophobic material in the center of the micelle with the water on the outside, the water is trapped in the center of the micelle. This exposes the hydrophobic tails to the SWCNTs which allow them to be more accessible for interactions with the gel. It has been showed by Strano et al. that the interaction between the SWCNT and the surfactant is between the hydrophobic tail and the SWCNT. This is due to the fact that the SWCNT is a carbonaceous material and is hydrophobic in nature. AOT differs greatly from SDS in that the twelve carbon tail in SDS is split into 2

tails in AOT, each tail having an ester before it reaches the sulfur head, allowing for better binding to the SWCNT.

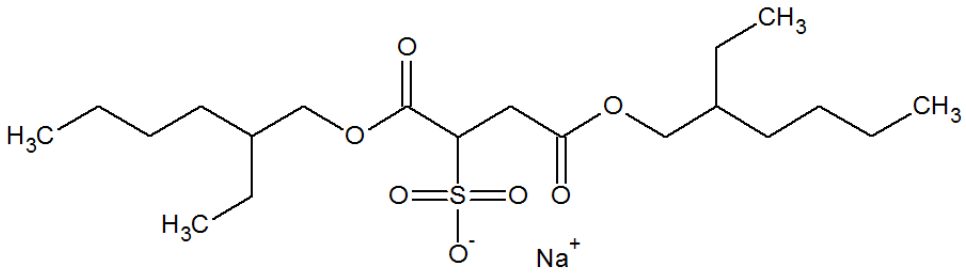

Dioctyl sulfosuccinate sodium (AOT)

Figure 3.7 – Representation of the AOT structure.

This reverse micelle arrangement of the AOT in solution allows for more interaction between the AOT and the SWCNT than is seen with the SDS. Running a column with SDS it is believed that the increase in concentration releases the SWCNTs because the SDS will interfere with the secondary amines on the Sephacryl, releasing the SWCNT. In order for SDS to interact with the SWCNT the micelle must be broken open to allow for the hydrophobic tails to interact with the SWCNT The interaction between the AOT and SWCNT is favorable because the hydrophobic tails are on the outside of the micelle. Because the relationship is believed to be a dynamic one where surfactant is continuously being added and removed from the SWCNT, the presence of AOT pushes the relationship in favor of the surfactant being on the SWCNT. This can be seen in a gradient column.

When a gradient was run from 0.33 mM to 7.99 mM it was observed that the majority of SWCNTs elute from the column at low concentrations. This can be seen when looking at the non-normalized map of AOT concentration vs absorbance (Figure 3.8, A). It is observed that after 0.99 mM very few SWCNTs elute from the column.

The map normalized at 780 nm of AOT concentration vs. absorbance (Figure 3.8, B) shows that at higher concentration of AOT small amount of smaller diameter SWCNTs elute from the column. At concentrations of 6mM and higher, smaller diameter SWCNT such as the (6,5) and (6,4) elute from the column but do so in very low concentrations. Between concentrations of 2 mM and 6 mM it was observed that there is a shift in the SWCNTs released from the gel. The absorbance pattern observed was similar to that seen when the column was run with SDS as the mobile phase.

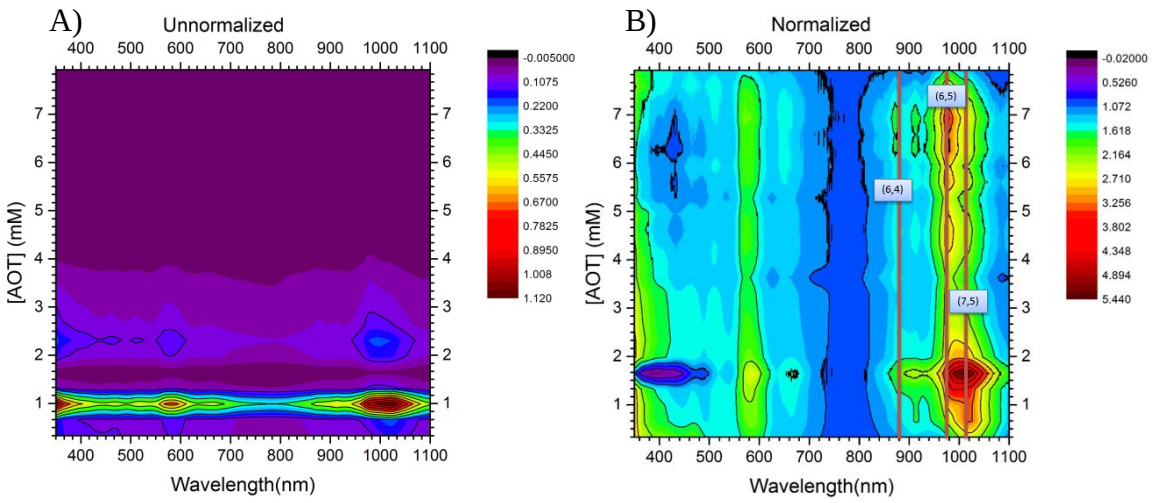

Figure 3.8 – A) Non-normalized illustration of absorbance data for AOT based gradient elution, B) normalized illustration of absorbance data for AOT based gradient elution.

To confirm that a shift in the SWCNTs released from the gel has occurred a column was run using 0.5 wt% SDS to elute the metallic SWCNTs from the column then 0.66 mM AOT to elute the first fraction of SWCNTs followed by 9 mM AOT to elute the rest of the SWCNTs (Figure 3.9).

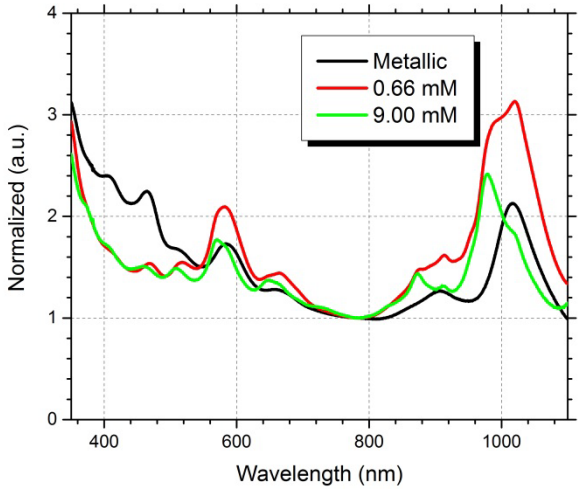

Figure 3.9 – Comparison of fractions collected from AOT gradient elution. The typical m-SWCNT fraction collected is also show for further comparison.

3.3.7 Peak analysis of AOT fractions

The resulting fractions show that a higher percentage larger diameter SWCNTs eluted from the column first. SWCNTs that preferentially elute in this fraction are the (7,5), (7,3), (9,1), (10,2) and (8,1) giving the fraction a blue-purple color. The second fraction, gray in color showed peaks for the (6,5), (6,4), (5,4), and (8,3), and this was confirmed with peak fitting and is shown in Figure 3.10.

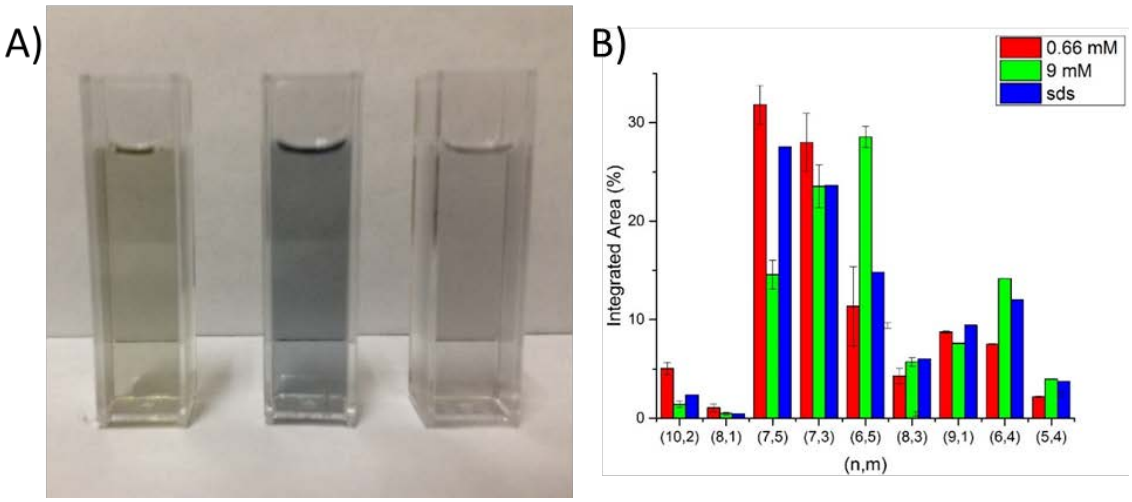

Figure 3.10 – A) Fractions after AOT separation, from left to right, fraction 1 eluted with 17mM SDS, fraction 2 eluted with 0.66 mM AOT and fraction 3 eluted with 9 mM AOT, B) integrated percentages of SWCNT (*n*,*m*) species in AOT gradient fractions.

From the peak fitting, the relative abundance of large diameter SWCNTs such as the (7,5) can be seen changing from 31.8 ±1.9 % to 14.5 ±1.5% and the (10,2) can be seen changing from 5.0 ± 0.6 % to 1.4 ± 0.3% (Figure 3.10). While smaller diameter SWCNTs such as the (6,5) and the (6,4) change from 11.4 ± 4.0% to 28.5 ± 1.1% and 7.5 ± 0.1% to 14.2 ± 0.1% respectively.

There is no trend when comparing the area %s to the chiral angle or E_{11} bandgap, but there was a correlation with the diameter of SWCNTs. (Appendix A2.). The (7,3) SWCNT does not follow the trend of larger diameter SWCNTs eluting before smaller diameter SWCNTs as it can be seen that the abundance dropped from 27.9 ± 2.9% to 23.5 ±2.1% with error that would allow for equal abundance of (7,3) in each fraction. This differs from the observed trend in that the (7,3) has a diameter of 0.706 nm and a chiral angle of 17°. Due to the small diameter it was expected that the (7,3) would elute in the second fraction but it was observed to elute with the first fraction at a high abundance.

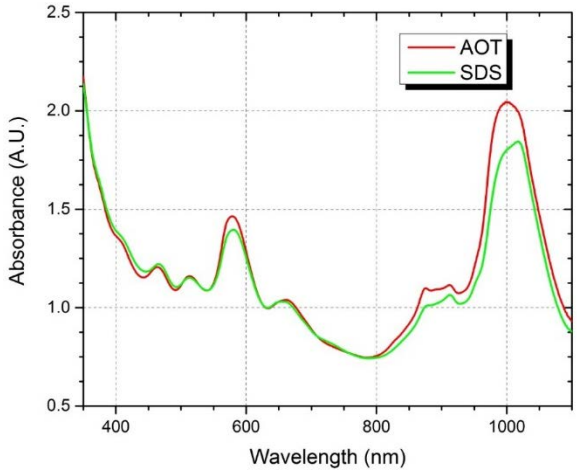

Figure 3.11- Total Semiconducting SWCNTs recovered by SDS and AOT through column chromatography using Sephacryl-S200.

AOT has shown to be able to produce enriched *(n,m)* fractions in a similar fashion as SDS. Using a mass absorptivity value of 0.043 L mg^{-1} cm^{-1} excepted by literature at a

wavelength of 763 nm the total amount of semiconducting SWCNTs recovered was able to be calculated for SDS and AOT to be 0.35 mg / 20 mL (Figure 3.11).[40] Because of the ability of AOT to recover the same amount of semiconducting SWCNTs as the SDS it is favorable as a surfactant for separation because of the reduction of overall cost needed to separate the SWCNTs. SDS commercially sells for $314.00 per kg from Sigma Aldrich while AOT sells for $116.00 per kg. Because lower concentrations of AOT on 9 mM AOT needed to produce the same separation as SDS and the overall cost of AOT being around one third the cost of SDS, AOT is a good chose when trying to produce *(n,m)* enriched samples.

3.3.8 Implications of AOT

While these results illustrate a number of important distinctions for the AOT as a positive choice for effective SWCNT separations, understanding the differences between its interactions versus those of SDS and SDBS are still an area of work that needs further exploration. One consideration is the differences in the Gibbs free energies for micelle formation, however, these values are within a few kJ/mol of each other: at 298 K -35, -32.5, and -33.2 kJ/mol for SDS, SDBS, and AOT, respectively.[54, 55] This means that for SDBS, it might be expected that free monomers may be more prevalent when compared to the other two surfactants and lead to an ability to remove the SWCNTs from the gel medium. However as reported here, SDBS has not been observed to allow an extensive removal of SWCNTs and the vast majority of material remained adsorbed on the column.

Another consideration is that the separation is kinetically, not thermodynamically constrained. The micellar structural sizes for these three surfactants are very different. SDS has an aggregation number of 60 - 80 at 298 K,[56] while SDBS and AOT are in the

range of ~20 and ~30, respectively.[56-58] It is thus proposed that a tightly bound spherical SDBS structure would have a more difficult time interacting strongly with the SWCNT/SDS micellar structure in the timescale of the direct addition of the SDBS as an eluent solution to the column.

While the AOT provides a similarly sized micelle structure as SDBS when it is isolated, its double-alkyl chains make it suitable to interact more readily with the SWCNT/SDS structures directly. In fact literature supports a positive interaction of AOT in the presence of other surfactants, leading to significantly higher aggregation numbers (> 50) in a mixed micelle environment.[59, 60] This means that potentially, on the timescale of flowing AOT eluent solution through the column, the AOT micelles break up into monomers or different structures that can coat the SWCNTs directly and thus overcome the binding affinity with the gel medium.

3.4 Conclusions

Separation of semiconducting SWCNTs into samples that are homogeneous for one (*n*,*m*) species of SWCNT are essential for the ability of SWCNTs to be integrated into many different applications. The new method described here demonstrates that varying the concentration of the mobile phase in a gel-based chromatography column will achieve similar results to those previously found in published literature using more elaborate techniques, such as multicolumn methods needing ultrasonication and ultracentrifugation. Lower affinity SWCNTs are weakly bound to the gel medium and only a small increase in the mobile phase concentration is needed to overcome the interactions. This method differs from other published methods as it allows for the creating of an enriched sample through the use of only a single column and can be done

in a rapid method. Notably, for the first time we illustrate the use of surfactants other than SDS in such a process.

The SDS gradient yields an enrichment of (6,5) SWCNTs at a concentration of SDS eluent at ~140 mM. There are important distinctive interactions between SDBS and AOT with the SWCNT/SDS micellar structures that result in significant changes in the ability of either surfactant to yield clean separated sc-SWCNTs. SDBS does not yield an appreciable quantity of separated SWCNTs, and this is believed to result from a slow kinetic exchange or interaction with the SWCNT/SDS structure. Interestingly, the AOT surfactant gradient achieves enriched sc-SWCNT material at very low concentrations (< 1 mM) and leads to an enriched quantity of the (7,5) SWCNT species. This indicates that with further refinements and understanding, one could tune a separation using surfactant and concentration to yield a specific SWCNT (*n*,*m*) species.

CHAPTER 4 – CONCLUSIONS AND FUTURE WORK

4.1 Conclusions

Fluorescence has been shown to be a valuable tool in the study of SWCNTs. However, in order to study the kinetics of SWCNT reactions, modifications to the standard florescence setup must be made to allow for the optimal amount of emission to be collected.

Working from the system designed by Rocha et al.[40] from Rice University, a portion of this work (Ch. 2) was focused on developing a system that allows for fast kinetic studies to be conducted. Using the LabVIEW programming platform a program controlling the new system was developed allowing for monitoring of the reaction kinetics and the ability to export the data to Origin data processing software. Fabrication of a mirror mount and sample holder allows for the focal point of the florescence to be relocated to the surface of the sample minimizing the re-absorbance of emission. The basic system operation was successfully tested with near-infrared fluorescent dyes, however, efforts to observe discernible near-infrared emission from a standard preparation of SWCNTs proved difficult.

Using the new fluorescence system developed for SWCNT kinetics, studies will be conducted that will answer questions presented in the current and previous separation studies. By understanding the interactions that occur during SWCNT separations, a method can be developed that will allow for industrial separation of the semiconducting SWCNTs to further the use of semiconducting SWCNTs for their electrical properties in future applications.

Separation studies using gel chromatography have shown that metallic SWCNTs can be easily separated from semiconducting SWCNTs on a scalable method because of the high affinity of the semiconducting SWCNTs to the Sephacryl gel, while the metallic SWCNTs have no affinity to the gel.

In a column of Sephacryl gel that allows semiconducting SWCNTs to adhere to the gel, the affinity of the different species of semiconducting SWCNTs can be exploited to better understand the role the surfactants plays in the separation of the samples.

In the primary results of this thesis (Ch. 3), it has been shown that the use of a concentration gradient of SDS, as well as, a previously unused surfactant (AOT) will elute more larger diameter SWCNTs from the column with low concentrations of surfactant while higher concentrations will elute more of the smaller diameter SWCNTs. It has been shown that the surfactant chosen has a direct effect on the ability to elute the sc-SWCNTs.

4.2 Future work

Future work on the near-IR spectrofluorimeter will start with the detection of the emission of a near-IR fluorescing dye in the inline system proposed in this thesis. First the investigation into the use of focusing mirrors will ensure that the excitation path of light will enter the aspheric lens true to the center of the lens, ensuring the focal spot is in the center of the lens so that the emission will be optimally collected by the aspheric lens. Focusing mirrors will allow for acute changes to be made to the excitation path without disrupting the whole system. This will also allow for the angle of the mirror to the sample holder to be greater than 45^0 allowing for more of the dichroic mirror to be used as a long pass filter ensuring that no excitation light reaches the detector.

Possible refabricating of the sample holder will ensure that the aspheric lens is mounted flush to the cuvette so that the emitted light flows along the same path that the excitation light takes. If the path of the emission is not in line with the excitation path then the dichroic mirror fails as a long pass filter.

After these issues are addressed, a focusing lens will be added in front of the detector to allow for the concentration of the emitted light onto the detecting surface. After confirming the emission of light with the near-IR emitting dye, the fluorescence of an unseparated sample of SWCNTs can be tested.

Once the emission of SWCNTs can be detected several studies can be done using the instrument to help understand the reactions happening in SWCNT separations. By observing the fluorescence quenching as SDS suspended SWCNTs interact with the gel medium we can understand if the interaction is between the SWCNT and the gel through any decrease in the intensity in fluorescence as gel is added into the sample. We can also observe the dynamics of the surfactant on the SWCNT as concentration is increased to understand why some species of SWCNT elute at low concentrations while others do not. Further, we can observe the effect of the addition of a competing surfactant to see if the surfactant being used in the separation is being replaced with the eluting surfactant. To achieve this, fluorescence in SWCNTs suspended in SDS can be monitored as the concentration of AOT is added to the sample.

One future direction for the gradient method of separation of SWCNTs, is to isolate the semiconducting species using a flash chromatography system or an HPLC to test the effect of a true gradient on the ability to elute SWCNTs. The method used in this study was a step gradient that will group different species of SWCNTs together if their

affinities are close to one another. Through the use of a true gradient, the separation of SWCNTs that are close to one another can be observed because it will allow for very small changes in concentration and will remove any experimental error in the preparation of the gradient.

After the use of a flash chromatography system or HPLC is conducted, the investigation of the effect different surfactants have on the ability to elute sc-SWCNTs can be investigated. Another surfactant that can be investigated is sodium cholate (SC), a surfactant that has been used in SWCNT separations by density gradient ultracentrifugation because of its ability to interact with semiconducting SWCNTs.[25]

Additionally, consideration for the kinetic interactions of SDBS, AOT, SC, or increased SDS on the SWCNT/SDS micellar structure could be probed using the spectrofluorimetric kinetic system or in a steady-state fluorimeter. With the expectation of the SWCNT/SDS structures bound to the gel medium resulting in diminished or quenched fluorescence, a baseline emission can be determined. Then the addition of the surfactants can be monitored directly or post addition as the SWCNTs desorb from the gel creating free SWCNT individuals in suspension. In particular, for the SDBS experiment, it may be that allowing the SDBS micelles an extended time to sit in the presence of the SWCNT/SDS-gel medium will lead to an increased amount of free SWCNTs, illustrating the possibility that the SDBS micelles are more tightly bound together and have a difficult time interacting with the SWCNT/SDS.

REFERENCES

1. Journet, C. M., W. K.; Bernier, P.; Loiseau, A.; de la Chapelle, M. L.; Lefrant, S.; Deniard, P.; Lee, R.; Fischer, J. E. . *Nature* **1997,** 388, 756-58.
2. Bronikowski, M. J.; Willis, P. A.; Colbert, D. T.; Smith, K. A.; Smalley, R. E. *Journal of Vacuum Science & Technology A: Vacuum, Surfaces, and Films* **2001,** 19, (4), 1800.
3. Bachilo, S. M. B., L.; Herrera, J. E.; Pompeo, F.; Resasco, D. E.; Weisman,R. B. *J. Am. Chem. Soc.* **2003,** 125, 11186-87.
4. Weisman, R. B.; Bachilo, S. M. *Nano letters* **2003,** 3, (9), 1235-1238.
5. White, C. T.; W., M. J. *J. Phys. Chem. B* **2005,** 109, 52-65.
6. Bachilo, S. M.; Strano, M. S.; Kittrell, C.; Hauge, R. H.; Smalley, R. E.; Weisman, R. B. *Science* **2002,** 298, 2361-2366.
7. Javey, A. *ACS nano* **2008,** 2, (7), 1329-35.
8. Jorio, A.; Dresselhaus, G.; dresselhaus, M. S., *Carbon Nanotubes- advanced topics in the sythesis, structure, properties and applications*. Springer: Berlin, 2008.
9. Weisman, R. B.; Bachilo, S. M. *Nano letters* **2003,** 3, (9), 1235-1238.
10. Strano, M. S.; Doorn, S. K.; Haroz, E. H.; Kittrell, C.; Hauge, R. H.; Smalley, R. E. *Nano letters* **2003,** 3, 1091-1096.
11. Lu, W.; Arthur, D. J.; Bartelt, N. C.; Berger, C.; Chen, W.; Conrad, E. H. *MRS Bulletin* **2012,** 37, (12), 1125-1135.
12. Bethune, D. S.; Klang, C. H.; De Vries, M. S.; Gorman, G.; Savoy, R.; Vazquez, J.; Beyers, R. *Nature* **1993,** 363, 605-07.
13. Thess, A. L., R.; Nikolaev, P.; Dai, H.; Petit, P.; Robert, J.; Xu, C.; Lee, Y. H.; Kim, S. G.; Rinzler, A. G.; Colbert, D. T.; Scuseria, G. E.; Tomanek, D.; Fischer, J. E.; Smalley, R. E. . *Science* **1996,** 273, 483-87.
14. Yakobson, B. I.; Smalley, R. E. *American Scientist* **1997,** 84, (4), 324-337.
15. Gamaly, G.; Ebbesen, T. W. *physical Review B* **1995,** 52, (3), 2083-2089.
16. Rigaku http://www.rigaku.co.jp/rms_en/application/appli02.html (4/31/2013),
17. Carbon, S. S.; Joselevich, E.; Lieber, C. M. *Nano* **2002,** 2, (1137-41).
18. www.intechopen.com http://www.intechopen.com/books/carbon-nanotubes-synthesis-characterization-applications/processing-carbon-nanotubes (4/31/2013).
19. Nikolaev, P.; Bronikowski, M. J.; Bradley, R. K.; Rohmund, F.; Colbert, D. T.; Smith, K. A.; Smalley, R. E. *Chemical Physics Letters* **1999,** 313, 91-97.
20. Kitiyanan, B.; Alvarez, W. E.; Harwell, J. H.; Resasco, D. E. *Chemical Physics Letters* **2000,** 317, 497-503.
21. Resasco, D. *SouthWest NanoTechnologies* **2011**, 1-6.
22. O'Connell, M. J.; Bachilo, S. M.; Huffman, C. B.; Moore, V. C.; Strano, M. S.; Haroz, E. H.; Rialon, K. L.; Boul, P. J.; Noon, W. H.; Kittrell, C.; Ma, J.; Hauge, R. H.; Weisman, R. B.; Smalley, R. E. *Science* **2002,** 297, 593-596.
23. www.intechopen.com http://www.intechopen.com/books/carbon-nanotubes-synthesis-characterization-applications/processing-carbon-nanotubes (4/31/2013).
24. Liu, H.; Nishide, D.; Tanaka, T.; Kataura, H. *Nature communications* **2011,** 2, 309.
25. Moshammer, K.; Hennrich, F.; Kappes, M. M. *Nano Research* **2009,** 2, (8), 599-606.

26. Carlson, L. J.; Krauss, T. D. *ACCOUNTS OF CHEMICAL RESEARCH* **2008,** 41, 235-243.
27. Arnold, D. *Nat. Nanotech* **2006,** 1, 60.
28. Hagen, A.; Hertel, T. *Nano letters* **2003,** 3, (3), 383-388.
29. Zhang, L.; Jia, Z.; Huang, L.; O'Brien, S.; Yu, Z. *J. Phys. Chem. C* **2007,** 111, (11240-11245).
30. Jiang, J.; Saito, R.; Sato, K.; Park, J.; Samsonidze, G.; Jorio, A.; Dresselhaus, G.; Dresselhaus, M. *Physical Review B* **2007,** 75, (3).
31. Jorio, A.; Saito, R.; Hafner, J.; Lieber, C.; Hunter, M.; McClure, T.; Dresselhaus, G.; Dresselhaus, M. *Physical Review Letters* **2001,** 86, (6), 1118-1121.
32. Lefebvre, J.; Homma, Y.; Finnie, P. *Physical Review Letters* **2003,** 90, (21).
33. Skoog; Holler; Crouch, *Principles of Instrumental Analysis*. 6th ed.; Thonson: Belmont,CA, 2007.
34. M.S. Dresselhaus; G. Dresselhaus; A. Jorio; A.G. Souza; M.A. Pimenta; Saito, R. *ACCOUNTS OF CHEMICAL RESEARCH* **2002,** 35, 1070.
35. Jost, O.; Gorbunov, A. A.; Pompe, W.; al., e. *Appl. Phys. Lett.* **1999,** 75, 2217.
36. Ohmori, S.; Saito, T.; Tange, M.; Shukla, B.; Okazaki, T.; Yumura, M.; Iijima, S. *J. phys. Chem. C* **2010,** 114, (22), 10077-10081.
37. Cherukuri, T. K.; Tsyboulski, D. A.; BruceWeisman, R. *ACS nano* **2012,** 6, (1), 843–850.
38. Cognet, L.; Tsyboulski, D. A.; Rocha, J. D.; Doyle, C. D.; Tour, J. M.; Weisman, R. B. *Science* **2007,** 316, (5830), 1465-8.
39. Kong, L.; Wang, J.; Fu, X.; Zhong, Y.; Meng, F.; Luo, T.; Liu, J. *Carbon* **2010,** 48, (4), 1262-1270.
40. Rocha, J. D.; Bachilo, S. M.; Ghosh, S.; Arepalli, S.; Weisman, R. B. *Analytical chemistry* **2011,** 83, (19), 7431-7.
41. Nair, N.; Kim, W.-J.; Braatz, R. D.; Strano, M. S. *Langmuir : the ACS journal of surfaces and colloids* **2008,** 24, (5), 1790-95.
42. Tanaka, T.; Jin, H.; Miyata, Y.; Kataura, H. *Applied Physics Express* **2008,** 1, 114001.
43. Hirano, A.; Tanaka, T.; Kataura, H. *The Journal of Physical Chemistry C* **2011,** 115, (44), 21723-21729.
44. Tvrdy, K.; Jain, R. M.; Han, R.; Hilmer, A. J.; McNicholas, T. P.; Strano, M. S. *ACS nano* **2013,** 7, (2), 1779-89.
45. Sciences, G. E. H. L. http://www.gelifesciences.com/webapp/wcs/stores/servlet/productById/en/GELifeSciences/17058401 (5/30/2014).
46. Silvera-Batista, C. A.; Scott, D. C.; McLeod, S. M.; Ziegler, K. J. *The Journal of Physical Chemistry C* **2011,** 115, (19), 9361-9369.
47. Jain, R. M.; Tvrdy, K.; Han, R.; Ulissi, Z.; Strano, M. S. *ACS nano* **2014,** 8, (4), 3367-3379.
48. Duque, J. G.; Densmore, C. G.; Doorn, S. K. *Journal of the American Chemical Society* **2010,** 132, (45), 16165-75.
49. Tummala, N. R.; Striolo, A. *ACS nano* **2009,** 3, (3), 595-602.
50. Fagan, J. A.; Zheng, M.; Rastogi, V.; Simpson, J. R.; Khripin, C. Y.; Batista, C. A. S.; Walker, A. R. H. *ACS nano* **2013,** 7, (4), 3373-3387.

51. Xu, Z.; Yang, X.; Yang, Z. *Nano letters* **2010,** 10, (3), 985-91.
52. Nair, N.; Usrey, M. L.; Kim, W.-J.; Braatz, R. D.; Strano, M. S. *Analytical chemistry* **2006,** 78, 7689-7696.
53. Tsyboulski, D. A.; Bachilo, S. M.; Weisman, R. B. *Nano letters* **2005,** 5, (5), 975-979.
54. Hait, S. K.; Majhi, P. R.; Blume, A.; Moulik, S. P. *The journal of physical chemistry. B* **2003,** 107, (15), 3650.
55. Chatterjee, a.; Moulik, S. P.; Sanyal, S. K.; Mishra, B. K.; Puri, P. M. *The journal of physical chemistry. B* **2001,** 105, (51), 12823.
56. Cheng, D. C. H.; Gulari, E. *journal of colloid and interface science* **1982,** 90, (2), 410.
57. Dey, J.; Bahattacharjee, J.; Hassan, P.; Aswal, V. K.; Das, S.; Ismail, K. *Langmuir* **2010,** 26, (20), 1592-15806.
58. Alargova, R. G.; Kochijashky, I. I.; Sierra, M. L.; Zana, R. *Langmuir* **1998,** 14, 5412.
59. Singh, O. G.; Ismail, K. *Journal of Surfactants and Detergents* **2008,** 11, (2), 89-96.
60. Mahajan, R. K.; Sharma, R. *Journal of colloid and interface science* **2011,** 363, (1), 275.

APPENDIX

A1. LabVIEW code

Laser control

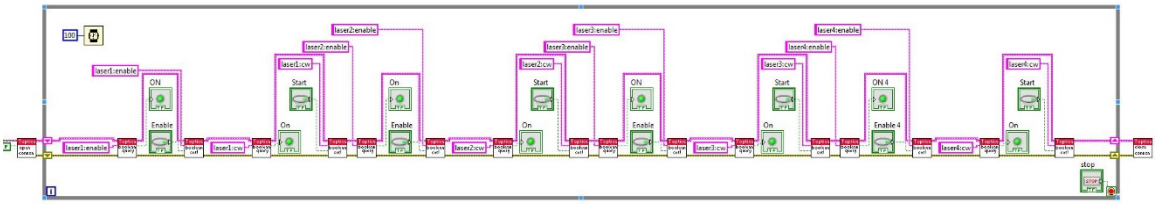

Data acquisition

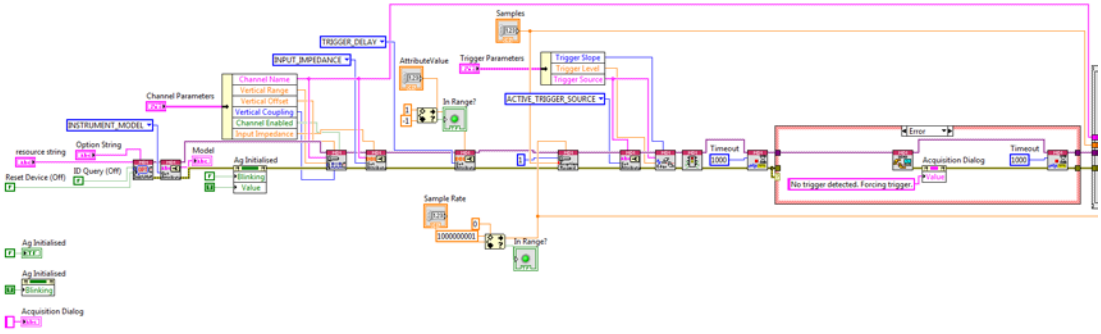

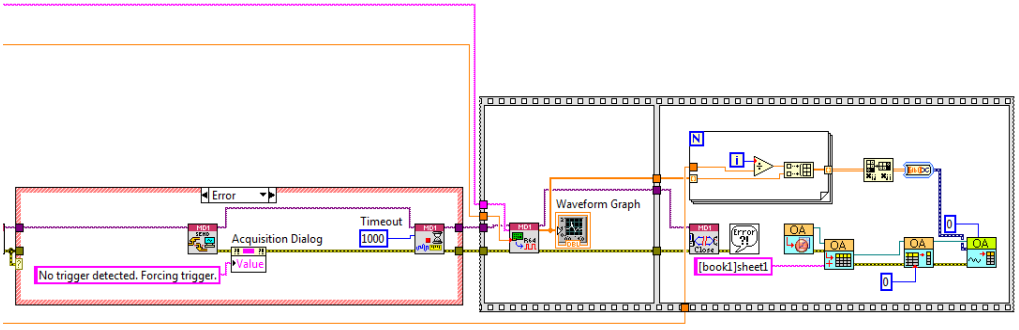

A2. Plots of SWCNT separations using AOT at two different concentrations, 0.66 mM and 9 mM.

A) Area %s vs diameter, B) Area %s vs chiral angle, C) Area %s vs E_{11}.

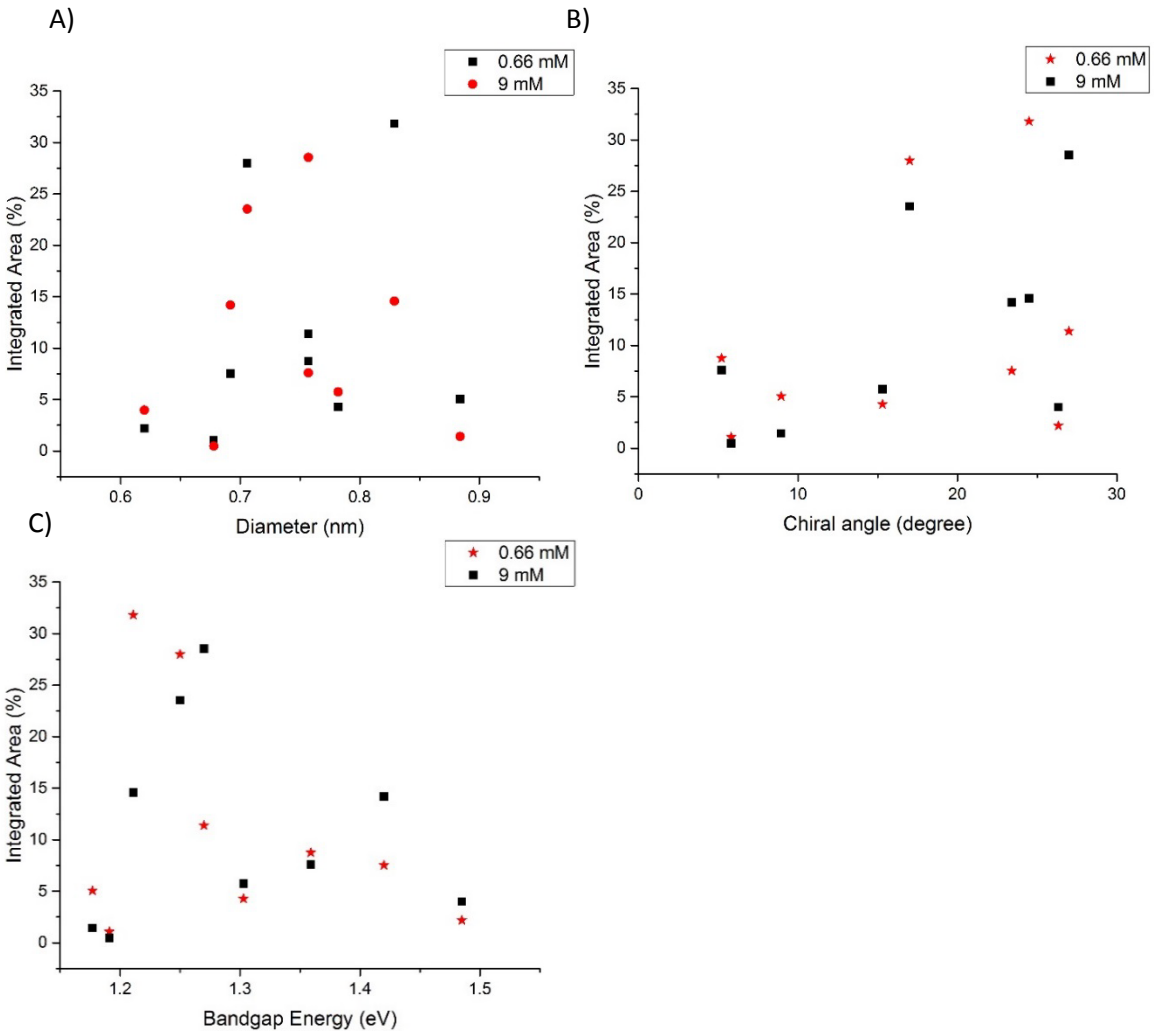

A3. SWeNT data sheets – SG65i

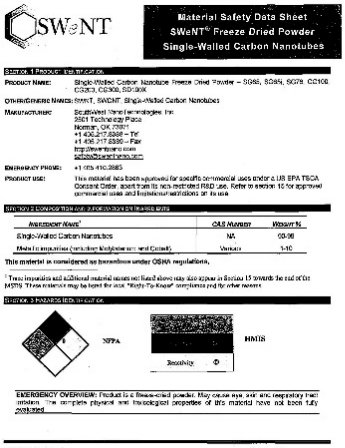

SWeNT

Material Safety Data Sheet
SWeNT® Freeze Dried Powder
Single-Walled Carbon Nanotubes

Section 1 Product Identification

PRODUCT NAME: Single-Walled Carbon Nanotubes Freeze Dried Powder – SG65, SG65i, SG76, CG100, CG300, CG300i, SG305

OTHER/SYNONYMS NAMES: SWeNT, SWCNT, Single-Walled Carbon Nanotubes

MANUFACTURER: SouthWest Nanotechnologies Inc
3501 Technology Place
Norman, OK 73071
+1 405.217.8388 – Tel
+1 405.217.8389 – Fax
http://swentsano.com
sales@swentsano.com

EMERGENCY PHONE: +1 ors 410.3965

PRODUCT USE: This material has been approved for specific commercial uses under a US EPA TSCA Consent Order apart from its less restricted R&D use. Refer to section 15 for approved commercial uses and limitations on its use.

Section 2 Composition and Information on Ingredients

Ingredient Name[1]	CAS Number	Weight %
Single-Walled Carbon Nanotubes	NA	90-98
Metal Impurities (residual catalyst as Fe and Co/Ni)	Various	1-10

This material is considered as hazardous under OSHA regulations.

[1] Trace impurities and additional material names not listed above may also appear in Section 15 towards the end of the MSDS. These materials may be listed the most "Widely Pre-Known" compliance and for other reasons.

Section 3 Hazards Identification

EMERGENCY OVERVIEW: Product is a freeze-dried powder. May cause eye, skin and respiratory tract irritation. The complete physical and toxicological properties of this material have not been fully investigated.

OSHA HAZARDS: Irritant
GHS LABEL ELEMENTS
PICTOGRAMS:
SIGNAL WORD: Warning
HAZARD STATEMENT(S)
H319: Causes serious eye irritation
H335: May cause respiratory irritation
PRECAUTIONARY STATEMENT(S)
P261: Avoid breathing dust/fume/gas/mist/vapours/spray
P305+P351+P338: If in eyes: Rinse cautiously with water for several minutes. Remove contact lenses, if present and easy to. Continue rinsing.

POTENTIAL HEALTH HAZARDS
SKIN: May cause skin irritation.
EYES: May cause eye irritation.
INHALATION: May cause irritation to the mucous membranes and upper respiratory tract. The product presents an increased inhalation hazard because of the small particle size.
INGESTION: Not a probable route of exposure. This material may be harmful if swallowed (e.g. unintentional hand-to-mouth transfer).
DELAYED EFFECTS: None known.

Ingredients found on one of the OSHA designated carcinogen lists are listed below.

Ingredient Name	NTP Status	IARC Status	OSHA List	ACGIH Status
Cobalt Compounds	Group 2[2]	2B[3]	None	A3[4]

[2] Reasonably anticipated to be human carcinogens
[3] Possibly carcinogenic to humans
[4] Confirmed animal carcinogen with unknown relevance to humans

Section 4 First Aid Measures

GENERAL: Contaminated clothing should be removed and washed before reused.
SKIN: Wash with soap and water. Get medical attention if irritation develops or persists.
EYES: Flush eyes with plenty of water for at least 15 min. Get medical attention if irritation develops or persists.
INHALATION: Remove to fresh air. If not breathing, give artificial respiration. Get medical attention if irritation develops or persists.
INGESTION: If person is conscious, rinse mouth with water. Do not induce vomiting unless directed to do so by a physician. Get medical attention immediately.
ADVICE TO PHYSICIAN: No specific advice. Treat symptomatically.

Section 5 Fire-Fighting Measures

Flash Point: Not applicable.

Respiratory Protection:
If there is potential for inhalation of dust, vapors, or aerosols wear a full-face NIOSH approved respirator with N100 cartridges or better.
The respirator must be selected based on contamination levels and use conditions found in the workplace. Use conditions must not exceed the working limits of the respirator. The respirator must be used in accordance with the OSHA respiratory protection standard (29 CFR 1910.134).
Hygiene Measures:
Keep away from foodstuffs, beverages and feed. Remove all soiled and contaminated material immediately. Wash hands before breaks and at the end of work.
Additional Recommendations:
Provide safety showers and eyewash stations in close proximity to the work area.
On-site Reportable Levels for Potential Decomposition Products: None.

Section 9 Physical and Chemical Properties

APPEARANCE:	Black powder		
PHYSICAL STATE:	Solid		
ODOR:	None		
SPECIFIC GRAVITY (water = 1.0):	0.114		
SOLUBILITY IN WATER (weight %):	Insoluble		
pH:	Not applicable		
BOILING POINT:	Not determined		
MELTING POINT:	3,652-6,062°C		
VAPOR PRESSURE:	Not determined		
VAPOR DENSITY (air = 1.0):	Not determined		
EVAPORATION RATE:	Not determined	COMPARED TO:	Not applicable.
% VOLATILES:	Not determined		
FLASH POINT[1]:	Not determined		

[1] Bulk powder ignition and additional flammability data are found in Section 5

Section 10 Stability and Reactivity

THERMAL DECOMPOSITION CONDITIONS TO AVOID:
Normally stable. Decomposition will not occur if used and stored according to specifications.
INCOMPATIBLE MATERIALS TO AVOID:
Strong oxidizing agents, acids, halogens, electrophiles, alkali metals.
HAZARDOUS DECOMPOSITION PRODUCTS:
Thermal decomposition products may include carbon monoxide, carbon dioxide and oxides of metallic impurities (including molybdenum and cobalt).

HAZARDOUS POLYMERIZATION:
Will not occur.

Section 11 Toxicological Information

IRRITATION (ACUTE) EFFECTS: No data available
DELAYED (SUBCHRONIC AND CHRONIC) EFFECTS: No data available
OTHER DATA: None

[1] Toxicological information on carbon nanotubes may be found at the website of International Council on Nanotechnology at http://cohesion.rice.edu/centersandinst/icon/.

Section 12 Ecological Information

No data available

[1] Information on ecological hazards can be found at the website of International Council on Nanotechnology at http://cohesion.rice.edu/centersandinst/icon/.

Section 13 Disposal Considerations

RCRA
Not classified as RCRA hazardous waste
OTHER DISPOSAL CONSIDERATIONS:
Except from small R&D samples, disposal of this product is not allowed by federal, state and local government regulations. It must be destroyed in hazardous waste incinerator and special care should be taken not to be released in the water.
NOTE: The information offered here is for the product as shipped. Use and/or alterations to the product such as mixing with other materials may significantly change the characteristics of the material and alter the RCRA classification and the proper disposal method.

Section 14 Transportation Information

US DOT HAZARD CLASS: Not regulated.
US DOT ID NUMBER: Not applicable.
For additional information on shipping regulations affecting this material, contact the information number found on Section 1.

Section 15 Regulatory Information

TOXIC SUBSTANCES CONTROL ACT (TSCA)
TSCA Inventory Status:
This material is manufactured according to the terms of TSCA consent order, for P08-810 C305 and should not be used for commercial purposes or in forms/forms used for commercial purposes, unless the recipient agrees in writing to comply with the requirements of the above consent order. As an exemption, the product can be further distributed only after it has been reacted in composites into an article or otherwise reduced into a physical form or state.
As a TSCA-cleared R&D substance, this product must be used by or directly under the supervision of technically qualified individual(s) as defined by TSCA, solely for R&D.

SWeNT

Certificate of Analysis

Material *SG65i*

Lot Number *SG65i-L39*

Parameter	*Specification*	*Measured Value*	*Measurement Method*
P2B	*≥ 5.5*	*6.68(@981nm)*	*UV-vis-NIR Spectroscopy*
S2B	*>0.75*	*0.83*	*UV-vis-NIR Spectroscopy*
(6,5) content (% of sc tubes)	*≥ 40*	*41*	*NS2*
Semiconducting tube Content (%)	*≥ 95*	*TBD*	*UV-vis-NIR Spectroscopy*
Residual Mass (%)	*<5*	*3.35*	*TGA*
Average diameter (nm)	*0.78±0.1*	*0.78*	*NS2*
Raman Q = (1-D/G)	*≥ 0.97*	*0.975*	*NS2*
Relative Purity (T1%)	*≥93*	*99.17*	*TGA*

TBD = to be determined

Information certified by:

Philip Wallis.

Philip Wallis
Director, Quality & Technical Support
SouthWest Nanotechnologies

DISCLAIMER: THE INFORMATION HEREIN IS PROVIDED IN GOOD FAITH, AND IS BELIEVED TO BE ACCURATE. NO WARRANTY, EXPRESSED OR IMPLIED, IS MADE REGARDING THE ACCURACY OR COMPLETENESS OF THIS INFORMATION.

Optical Absorbance Spectrum – Lot# SG65i-L39

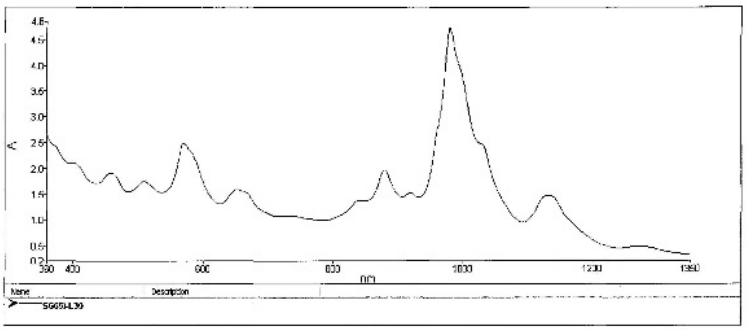

Thermogravimetric Analysis – Lot# SG65i-L39

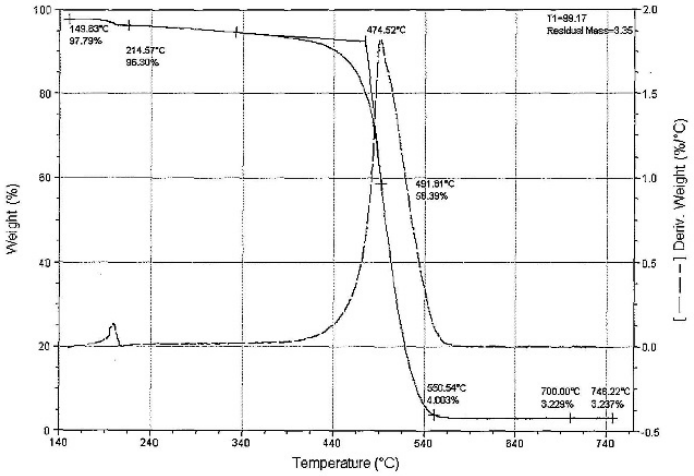

Raman Spectrum – Lot# SG65i-L39

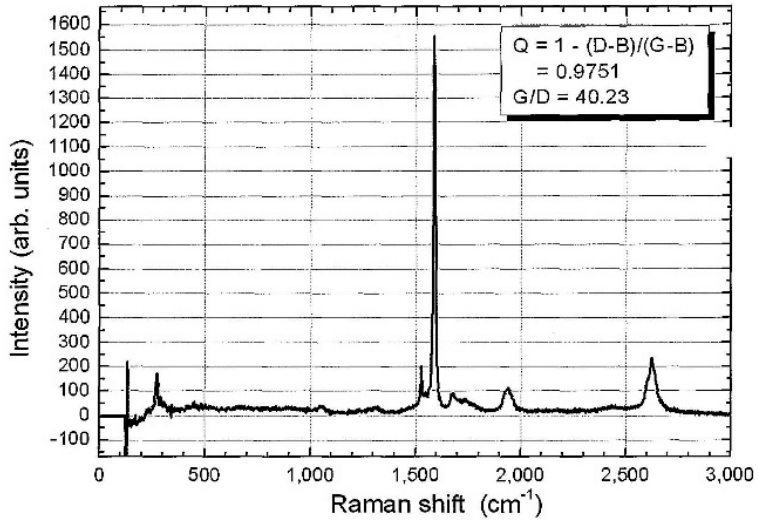

Chiral Distribution – Lot# SG65i-L39

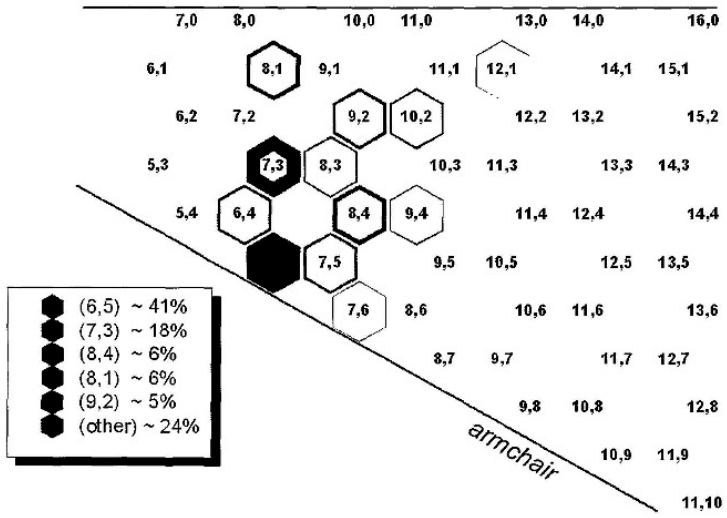

Diameter Distribution – Lot# SG65i-L39